QSO重力レンズ多重像のフラックス異常問題に対する視線方向のダークハローの影響について

Kaiki Taro Inoue (KINDAI)
Ryuichi Takahashi (Hirosaki U.)

refs: Inoue & Takahashi 2012, MNRAS in press, arXiv:1207.2139
Takahashi & Inoue 2012, in preparation

Flux- ratio anomalies

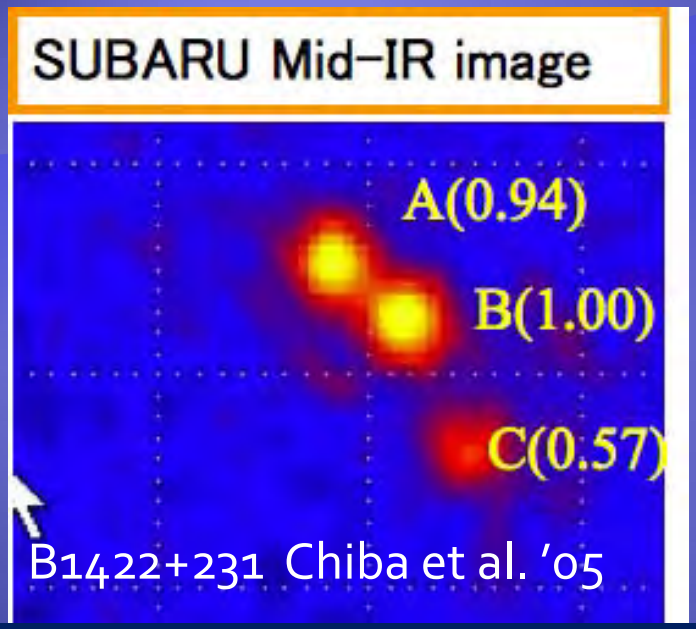

- Positions can be well fit to the model.
- Flux-ratios fits are poor.

Cusp-caustic relation

$$\frac{A+B+C}{|A|+|B|+|C|}=0$$

(Mao & Schneider ' 98 Metcalf & Madau '01, Chiba ' 02, Dalal & Kochanek' 02)

Flux- ratio anomalies

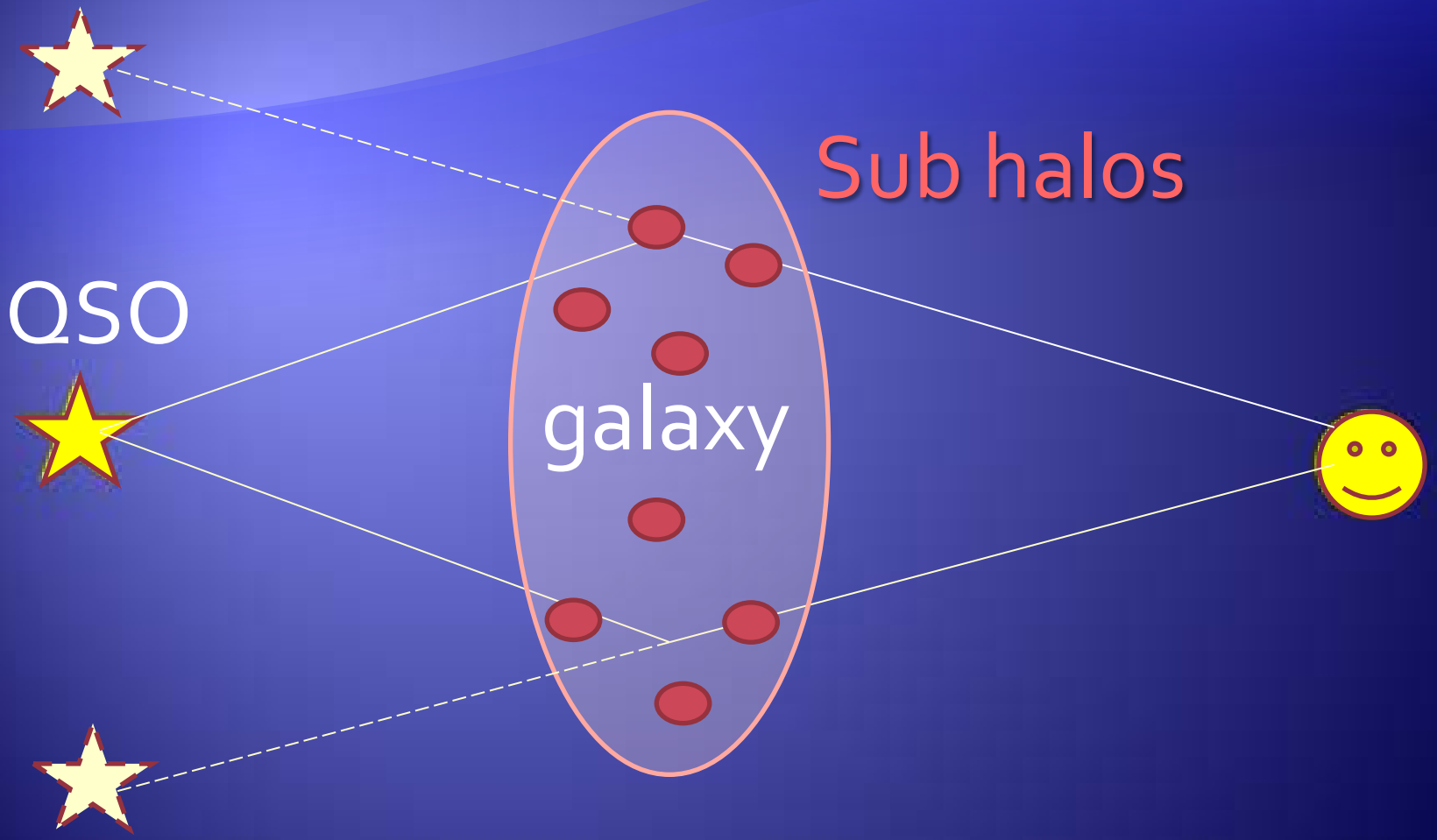

Flux- ratio anomalies

- Sub halos

  but predicted subhalos too low for anomalies

  (Maccio & Mirranda 2006, Amara et al. 2006;
  Xu et al. 2009, 2010; Chen 2009; Chen et al. 2011)

- Luminous satellites may contribute significantly

  (McKean et al. 2007, Shin & Evans 2008;
  MacLeod et al. 2009)

- Line-of-sight halos?

  (Chen et al. 2003, Metcalf 2005, Xu et al. 2011)

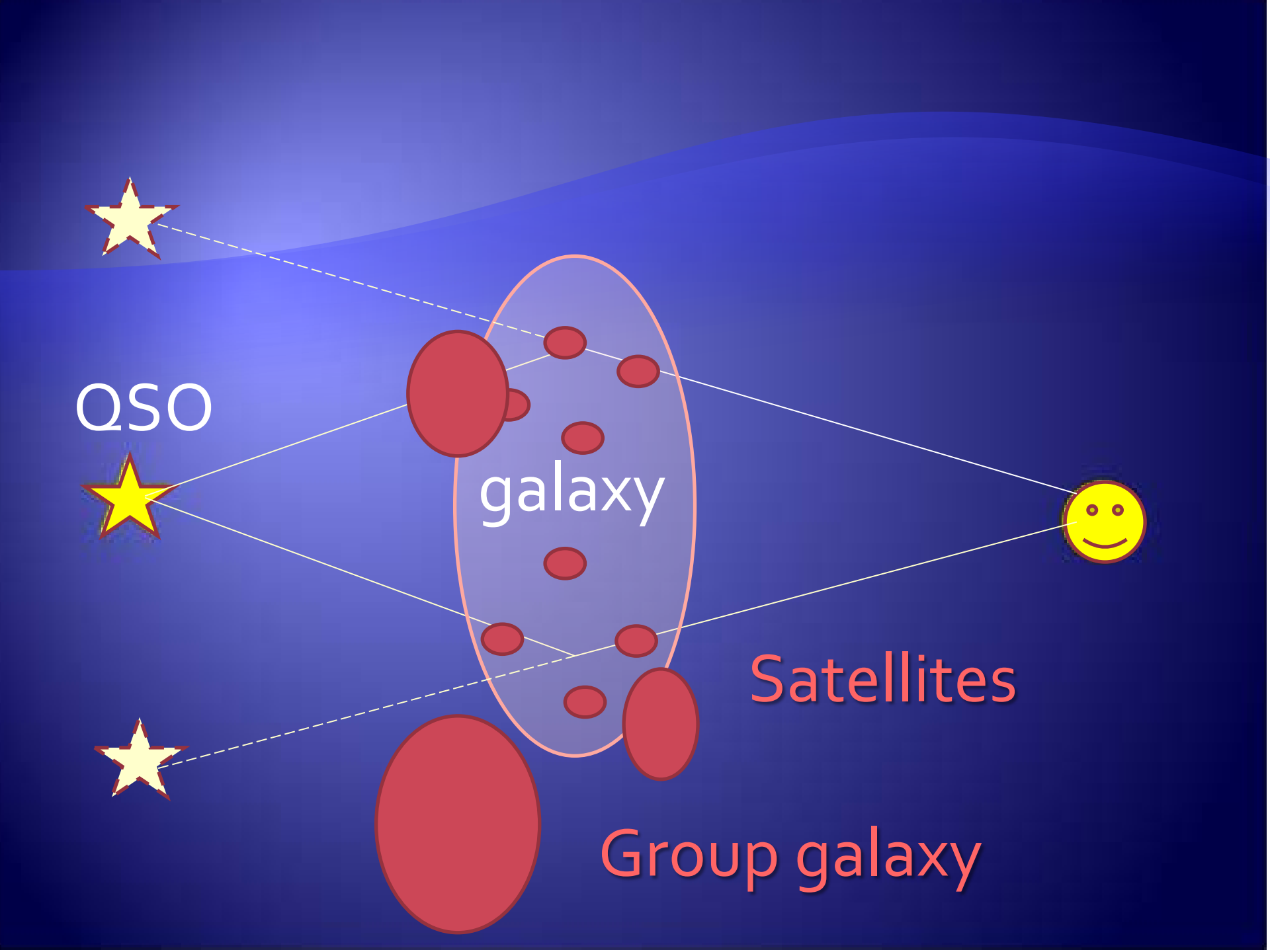
QSO
galaxy
Satellites
Group galaxy

Flux- ratio anomalies

- Sub halos

  but predicted subhalos too low for anomalies

  (Maccio & Mirranda 2006, Amara et al. 2006;
  Xu et al. 2009, 2010; Chen 2009; Chen et al. 2011)

- Luminous satellites may contribute significantly

  (McKean et al. 2007, Shin & Evans 2008;
  MacLeod et al. 2009)

- Line-of-sight halos?

  (Chen et al. 2003, Metcalf 2005, Xu et al. 2011)

Flux- ratio anomalies

- Sub halos

  but predicted subhalos too low for anomalies

  (Maccio & Mirranda 2006, Amara et al. 2006;
  Xu et al. 2009, 2010; Chen 2009; Chen et al. 2011)

- Luminous satellites may contribute significantly

  (McKean et al. 2007, Shin & Evans 2008;
  MacLeod et al. 2009)

- Line-of-sight halos?

  (Chen et al. 2003, Metcalf 2005, Xu et al. 2011)

Flux- ratio anomalies

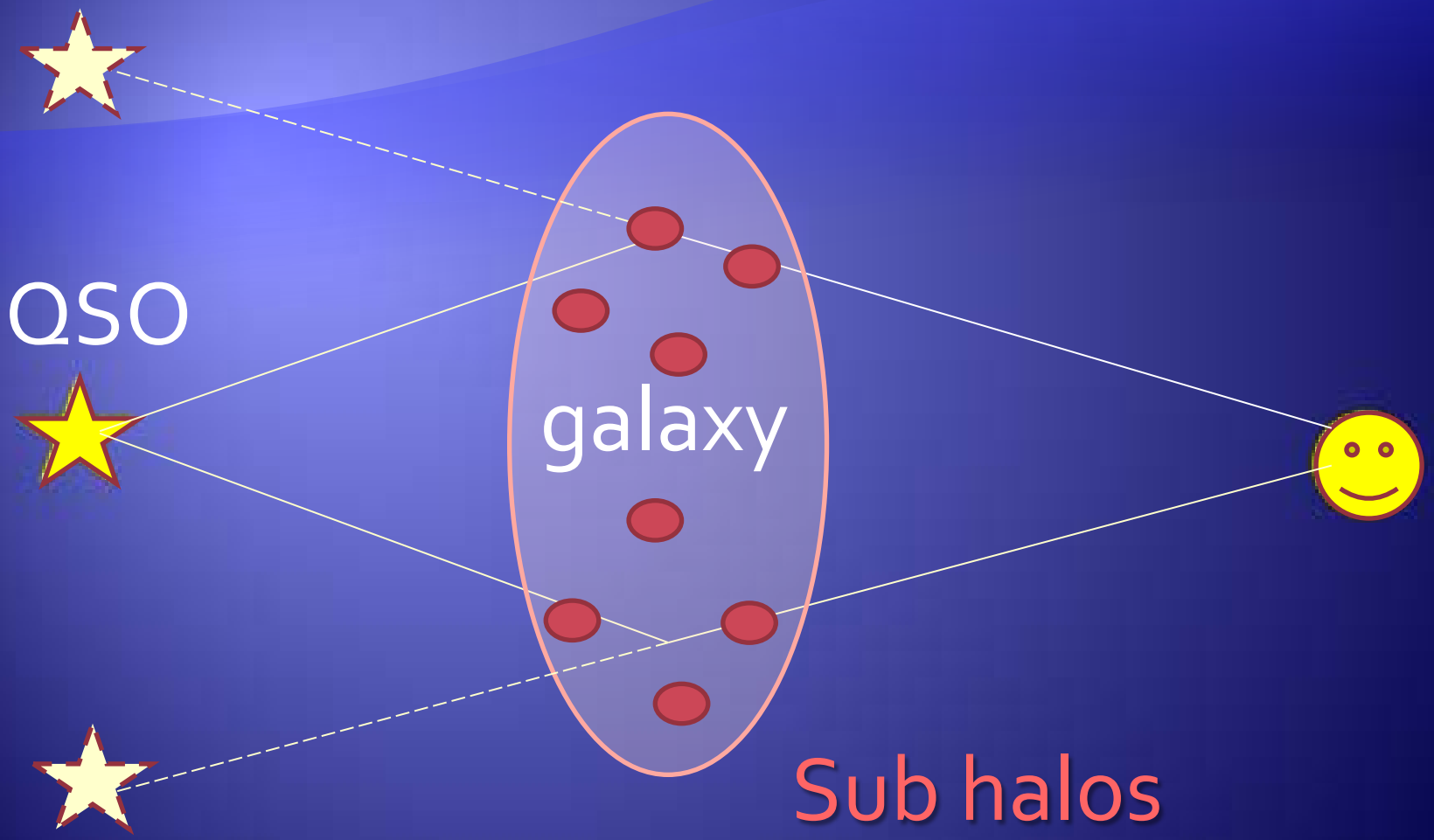

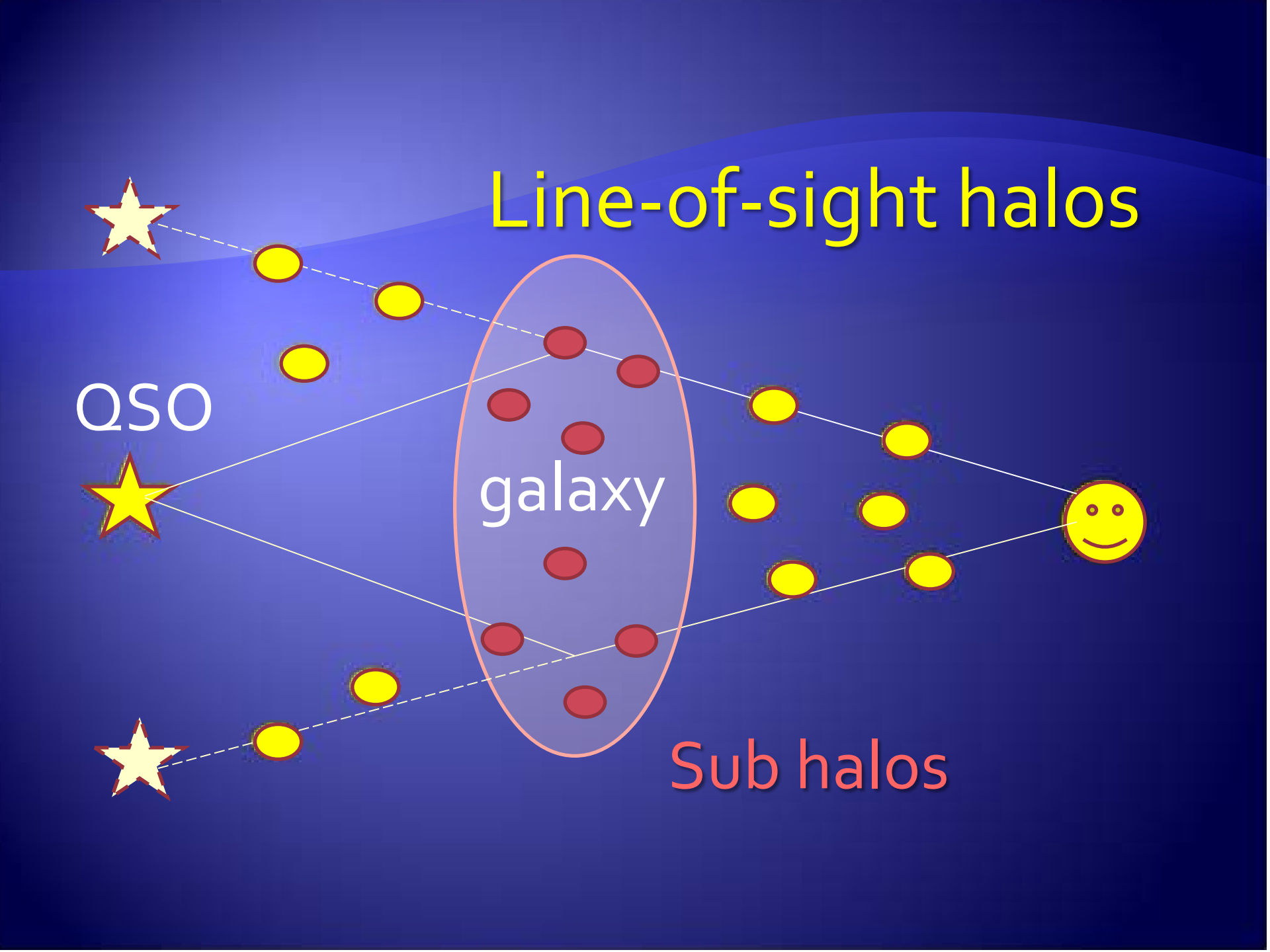
Line-of-sight halos
QSO
galaxy
Sub halos

6 MIR quadruple lenses

Table 1. Observed MIR Flux Ratios

Lens	z_L	z_S	N	Flux Ratio			$\langle\epsilon\rangle$ ($''$)	$\langle\theta\rangle$ ($''$)	Reference
RXJ1131-1231($\star$)				A/B	C/B				
	0.295	0.658	3	$1.63^{+0.04}_{-0.02}$	$1.19^{+0.03}_{-0.12}$		0.017	1.9	1, 2
Q2237+0305				B/A	C/A	D/A			
	0.04	1.695	4	0.84 ± 0.05	0.46 ± 0.02	0.87 ± 0.05	0.0046	0.9	1, 3
PG1115+080				A2/A1					
	0.31	1.72	2	0.93 ± 0.06			0.020	1.2	1, 4
H1413+117				B/A	C/A	D/A			
	1.88($\star\star$)	2.55	4	0.84 ± 0.07	0.72 ± 0.07	0.40 ± 0.06	0.020	0.6	5
MG0414+0534				A2/A1	B/A1				
	0.96	2.639	3	0.90 ± 0.04	0.36 ± 0.02		0.0042	1.2	1, 3
B1422+231				A/B	C/B				
	0.34	3.62	3	0.94 ± 0.05	0.57 ± 0.06		0.0042	1.1	1, 4

References:1. CASTLES; 2. Sugai et al. 2007; 3. Minezaki et al. 2009; 4. Chiba et al. 2005; 5. MacLeod et al. 2009

Note: ($\star$): [OIII] line flux ratios. ($\star\star$): The lens redshift z_L is obtained from a best-fit model using the observed positions of the images and the primary lens, the flux ratios, and the time-delays between the images assuming $H_0 = 70\,\mathrm{km/s/Mpc}$.

Our work

- Semi-analyitic estimate based on VERY high resolution N-body simulation fully incorporating clustering effects of M>10^5 solar mass halos
- Astrometric shifts taken into account
- New static rather than 'classic' cusp-caustic relations
- Only MIR lenses. Source sizes =O[1 pc]

Magnification perturbation

singular isothermal elliposoid（SIE）+ external shear model で像の位置を再現

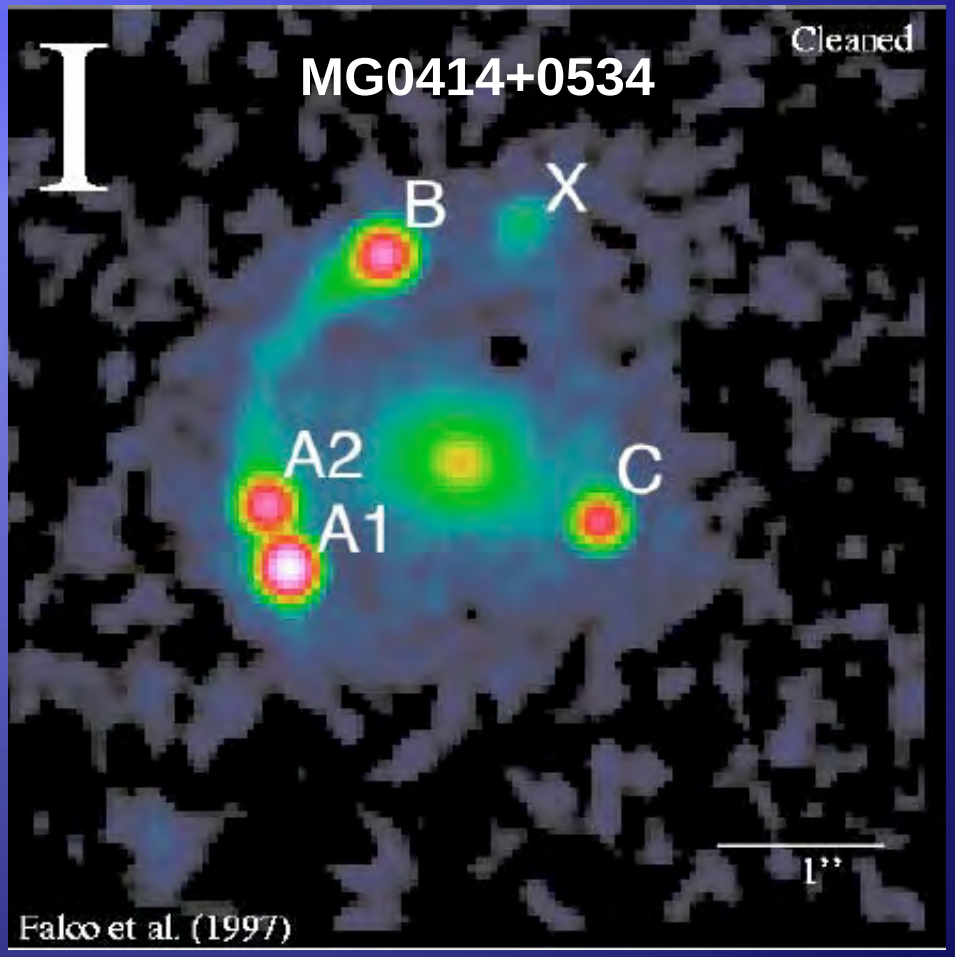

各像での convergence κ, shear $\gamma_{1,2}$, magnification μ を求める

Magnification perturbation

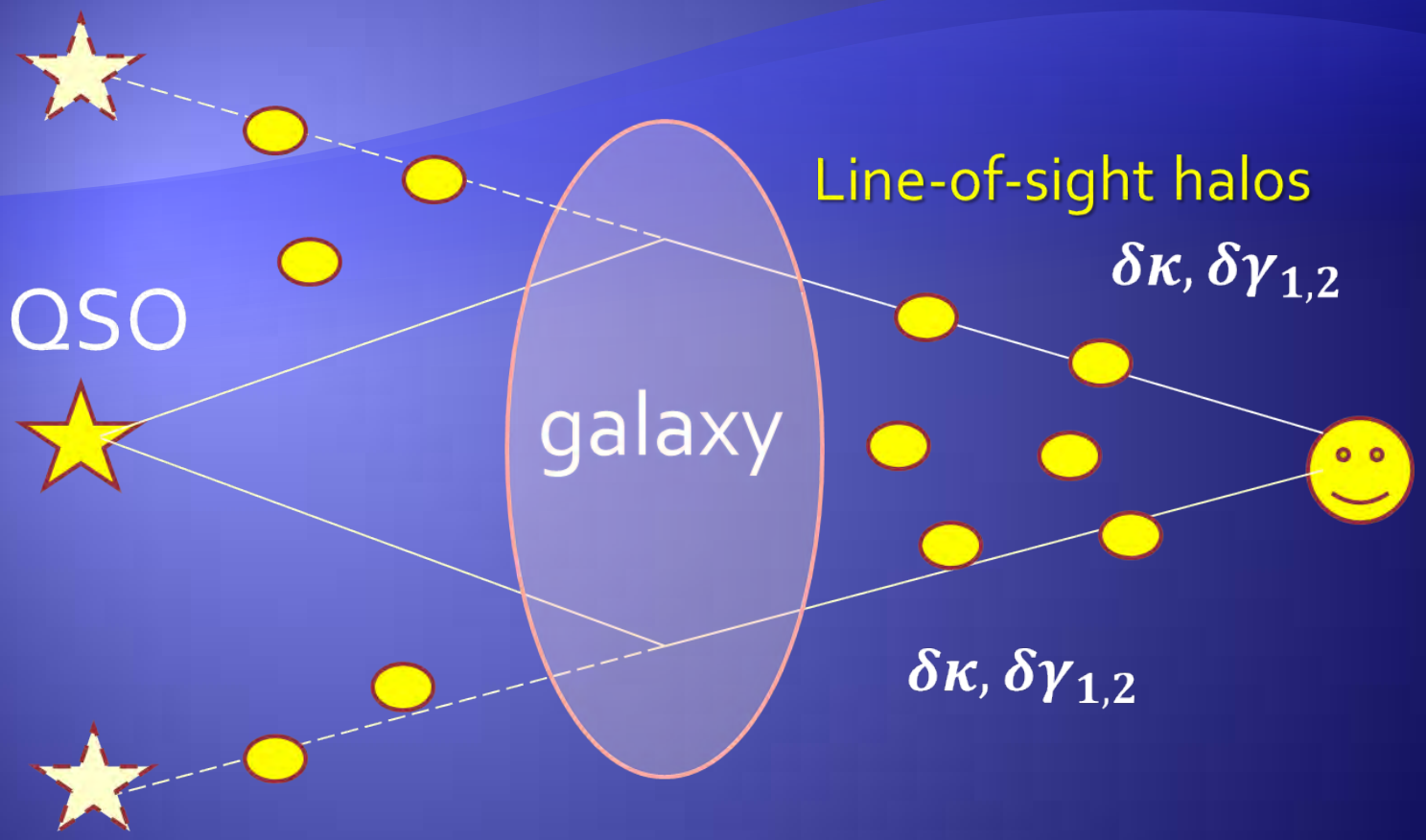

視線方向のダークハローによる寄与を加える

$$\kappa \to \kappa + \delta\kappa, \quad \gamma_{1,2} \to \gamma_{1,2} + \delta\gamma_{1,2}$$

$$\mu \to \mu + \delta\mu$$

New statistic η

A,C: minimum B:saddle, $\kappa_B < 1$

$$\delta_i^{\mu} \equiv \delta\mu_i / \mu_i .$$

:magnification contrast

η: effective magnification perturbation

$$\eta^2(\mathrm{A,B,C}) = \frac{1}{4}[(\delta_A^{\mu} - \delta_B^{\mu})^2 + (\delta_C^{\mu} - \delta_B^{\mu})^2].$$

$$\eta^2 \approx \frac{1}{4}\left[\left(\frac{AB_0}{A_0B} - 1\right)^2 + \left(\frac{CB_0}{C_0B} - 1\right)^2\right].$$

B1422+231

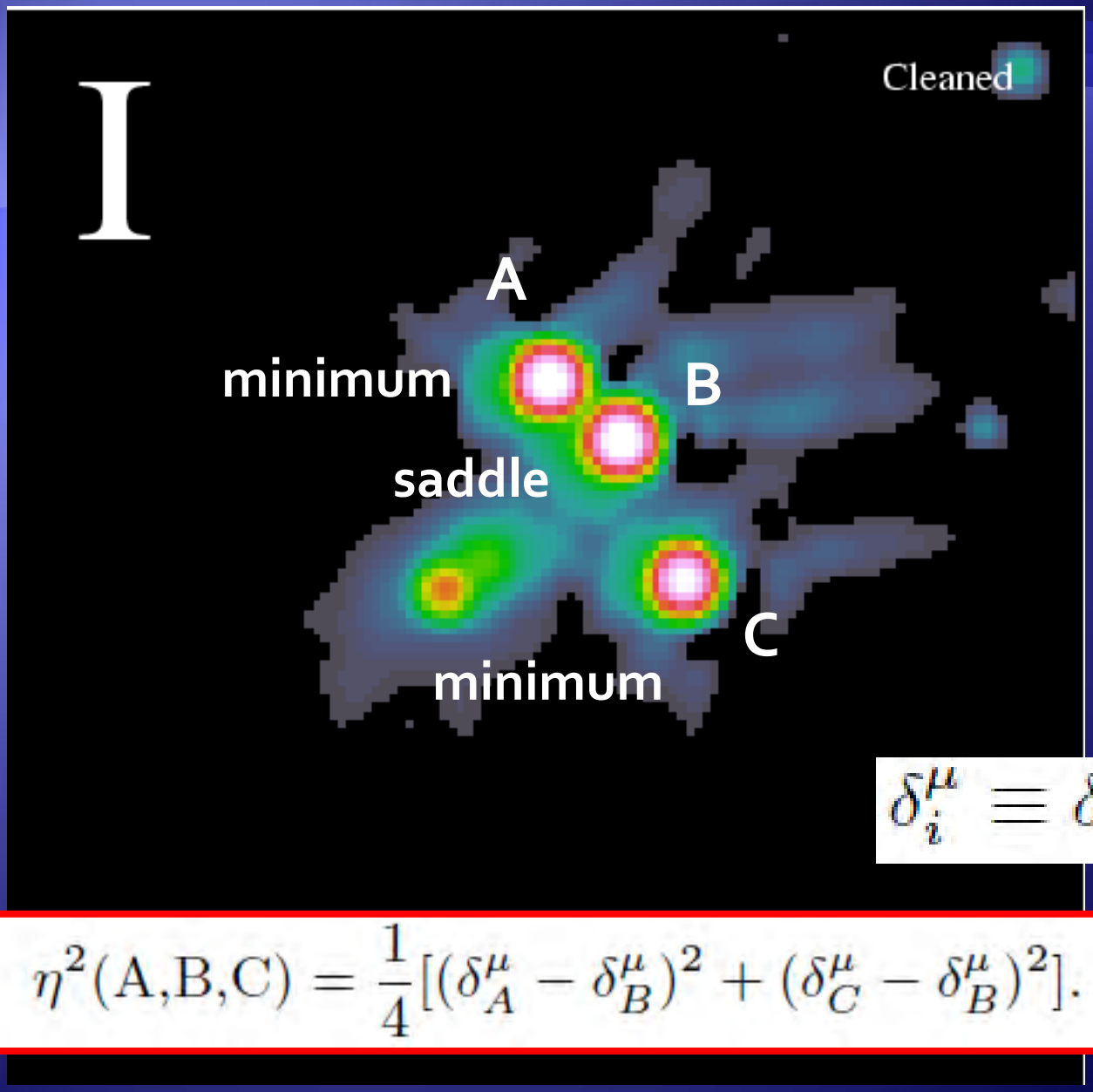

$$\delta_i^{\mu} \equiv \delta\mu_i / \mu_i .$$

$$\eta^2(\mathrm{A,B,C}) = \frac{1}{4}[(\delta_A^{\mu} - \delta_B^{\mu})^2 + (\delta_C^{\mu} - \delta_B^{\mu})^2].$$

New statistic η

$$\langle \eta^2 \rangle = \frac{1}{4}\Big[(J_A + J_B)\sigma_\kappa^2(0) - 2J_{AB}\xi_\kappa(\theta_{AB}) + (J_B + J_C)\sigma_\kappa^2(0) - 2J_{BC}\xi_\kappa^2(\theta_{BC})\Big],$$

where

$$J_i = \mu_i^2(4(1-\kappa_i)^2 + 2\gamma_i^2),$$

and

$$J_{ij} = \mu_i\mu_j(4(1-\kappa_i)(1-\kappa_j) + 2\gamma_i\gamma_j),$$

κ: background convergence γ: background shear

Constrained 2-point correlation

$$\begin{aligned}
\xi_\kappa(\theta) &\equiv \langle \delta\kappa(0)\delta\kappa(\theta)\rangle \\
&= \frac{9H_0^4\Omega_{m,0}^2}{4c^4}\int_0^{r_S} dr r^2\left(\frac{r-r_S}{r_S}\right)^2[1+z(r)]^2 \\
&\times \int_0^\infty \frac{dk}{2\pi} kW(k;k_{cut}(r;\epsilon))P_\delta(k;r)J_0(g(r)k\theta),
\end{aligned}$$

Dark matter の揺らぎの power spectrum

MG0414+0534

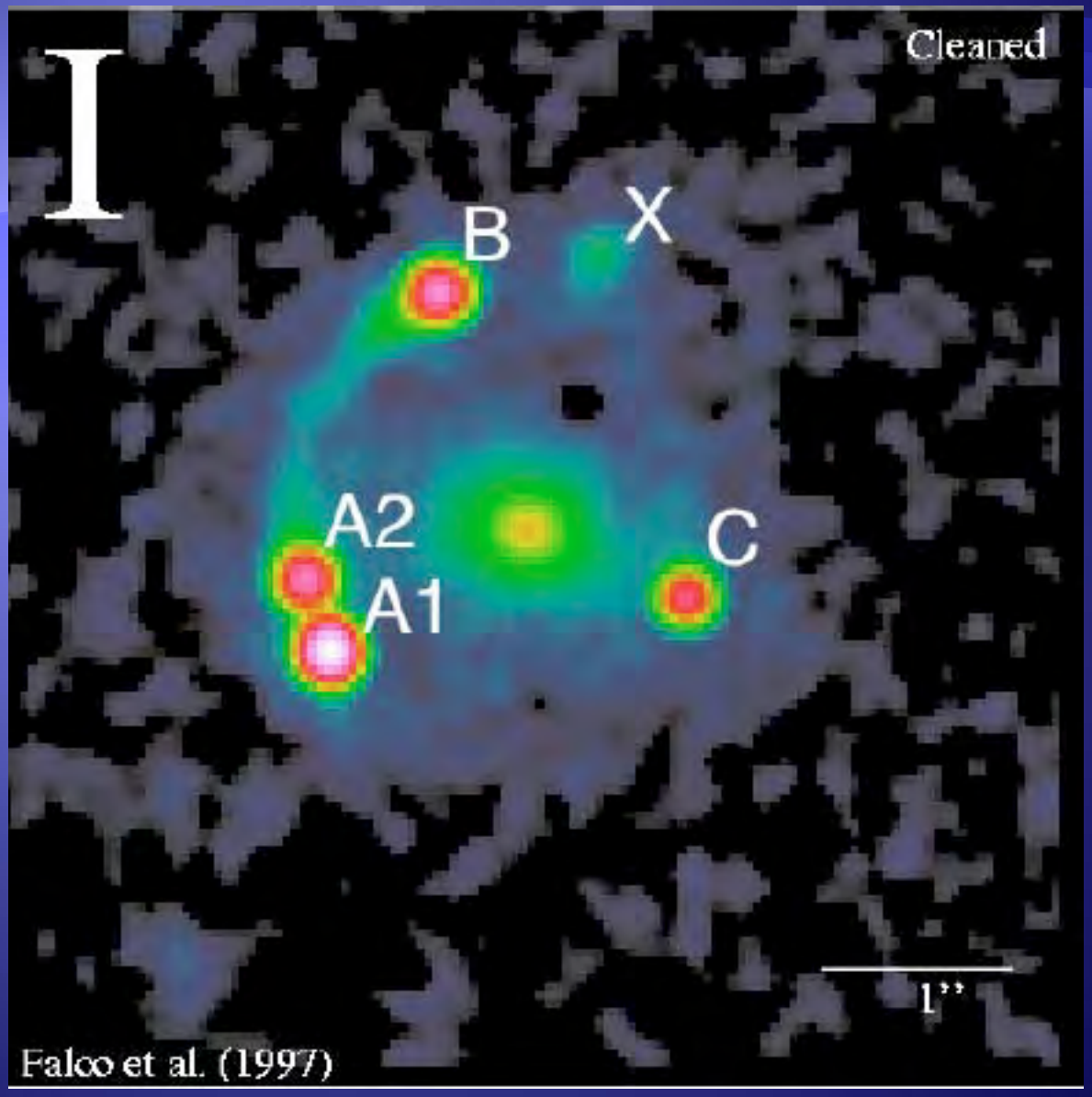

MG0414+0534

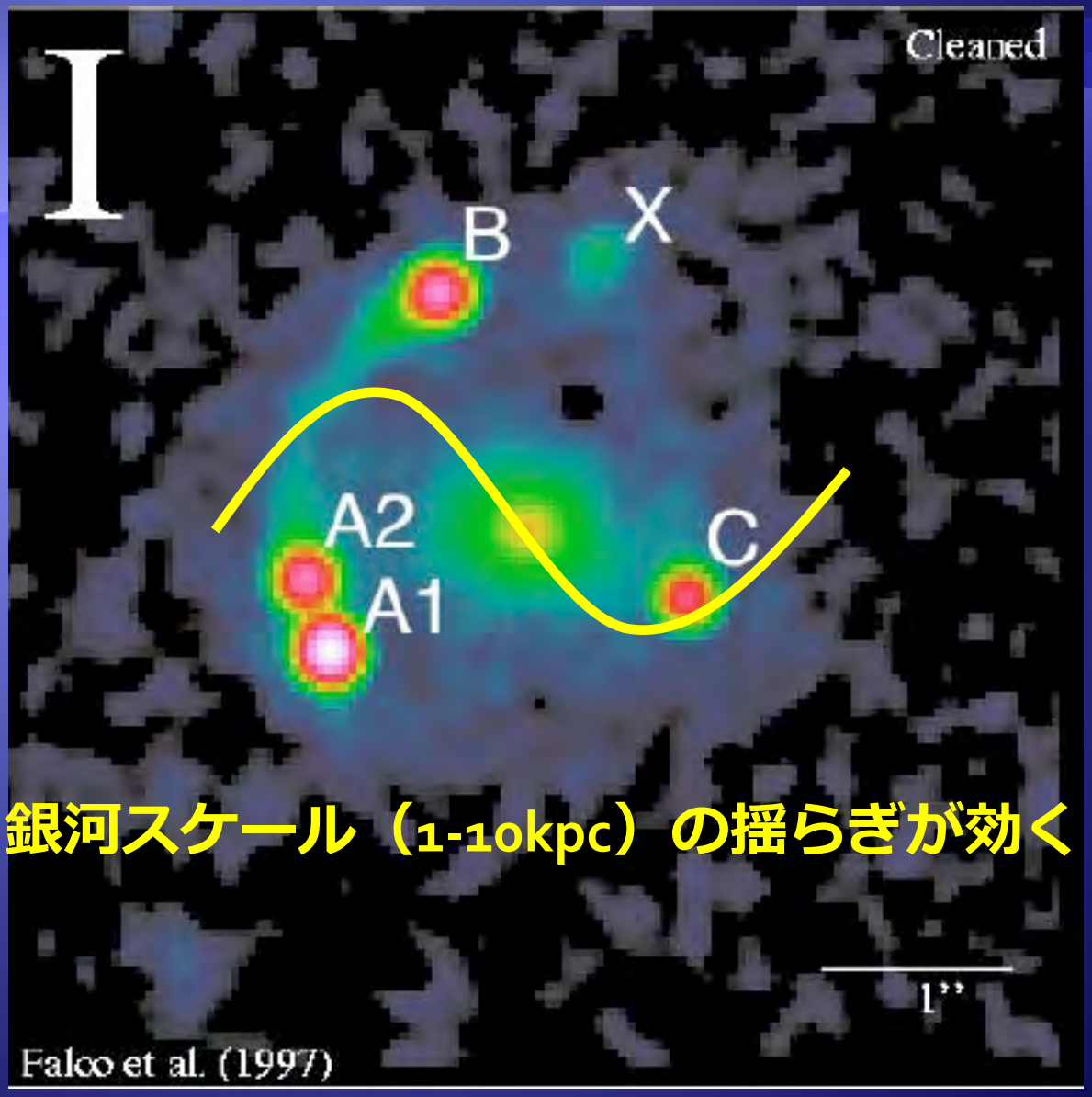

銀河スケール（1-10kpc）の揺らぎが効く

Astrometric shifts

$$2\langle\delta\theta^2(0)\rangle - 2\langle\delta\theta(0)\delta\theta(\theta_{AB})\rangle < \epsilon^2,$$

Given by accuracy in position of centroid ε

Minimum wavenumber given by ε

$$k_\varepsilon = O[100h/\mathrm{Mpc}]$$

Non-linear power spectrum

N-body Simulation

- Two 512^3 one 1024^3 colissionless particles simulations :baryons are not included.
- Box-size=10Mpc/h code: L-Gadget (Springel et al.)
- Plus simulations with box-size=320,800,2000Mpc/h
- HITACHI SR16000 512CPUs, CPU time >3 months
- Concordant LCDM (WMAP7yr+H_0+BAO)

Non-linear power spectrum

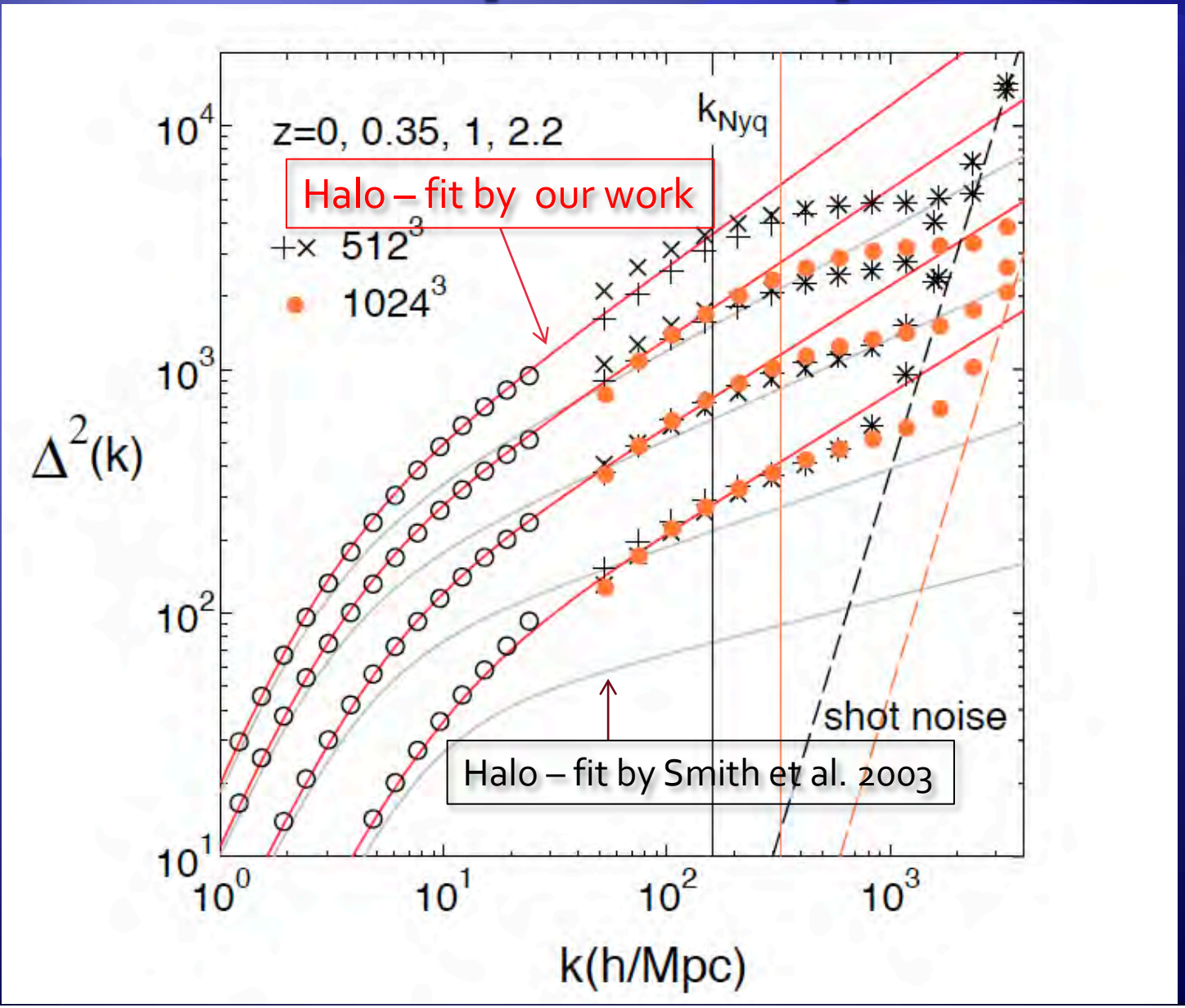

Non-linear power spectrum

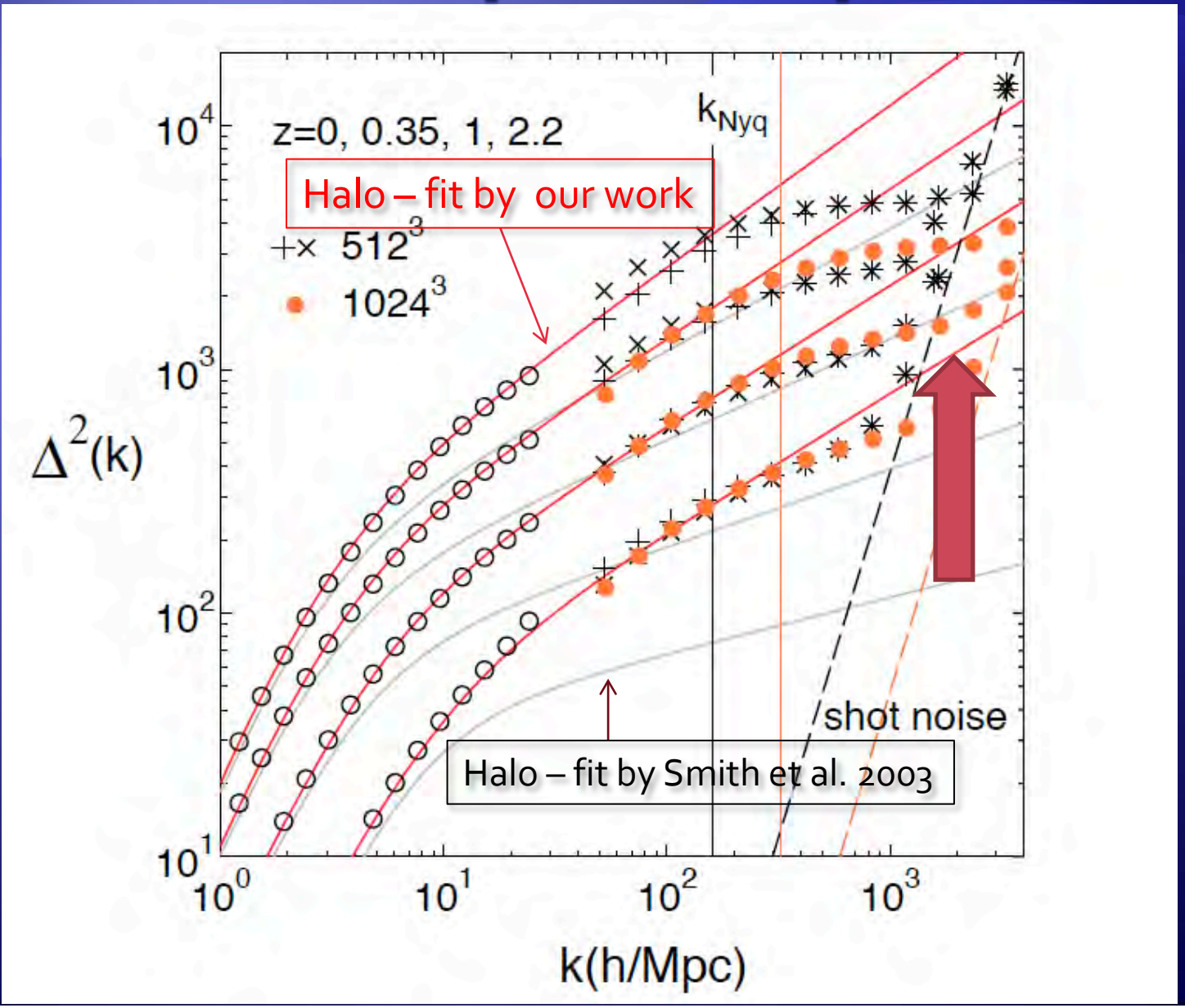

Application to MIR lenses

MIR QSO-galaxy quads

- 6 samples:5 continuum 1 line [OIII]
- SIE-ES model possibly with SIS for a luminous satellite (gravlens by Keeton)
- Astrometric shifts given by position errors (CASTLES) in lensed images and lens & size of critical curves -> minimum wavelength.

MIR quadruple lenses

Table 1. Observed MIR Flux Ratios

Lens	z_L	z_S	N	Flux Ratio			$\langle\epsilon\rangle$ ($''$)	$\langle\theta\rangle$ ($''$)	Reference
RXJ1131-1231($\star$)				A/B	C/B				
	0.295	0.658	3	$1.63^{+0.04}_{-0.02}$	$1.19^{+0.03}_{-0.12}$		0.017	1.9	1, 2
Q2237+0305				B/A	C/A	D/A			
	0.04	1.695	4	0.84 ± 0.05	0.46 ± 0.02	0.87 ± 0.05	0.0046	0.9	1, 3
PG1115+080				A2/A1					
	0.31	1.72	2	0.93 ± 0.06			0.020	1.2	1, 4
H1413+117				B/A	C/A	D/A			
	1.88($\star\star$)	2.55	4	0.84 ± 0.07	0.72 ± 0.07	0.40 ± 0.06	0.020	0.6	5
MG0414+0534				A2/A1	B/A1				
	0.96	2.639	3	0.90 ± 0.04	0.36 ± 0.02		0.0042	1.2	1, 3
B1422+231				A/B	C/B				
	0.34	3.62	3	0.94 ± 0.05	0.57 ± 0.06		0.0042	1.1	1, 4

References:1. CASTLES; 2. Sugai et al. 2007; 3. Minezaki et al. 2009; 4. Chiba et al. 2005; 5. MacLeod et al. 2009

Note: ($\star$): [OIII] line flux ratios. ($\star\star$): The lens redshift z_L is obtained from a best-fit model using the observed positions of the images and the primary lens, the flux ratios, and the time-delays between the images assuming $H_0 = 70\,\mathrm{km/s/Mpc}$.

Result I

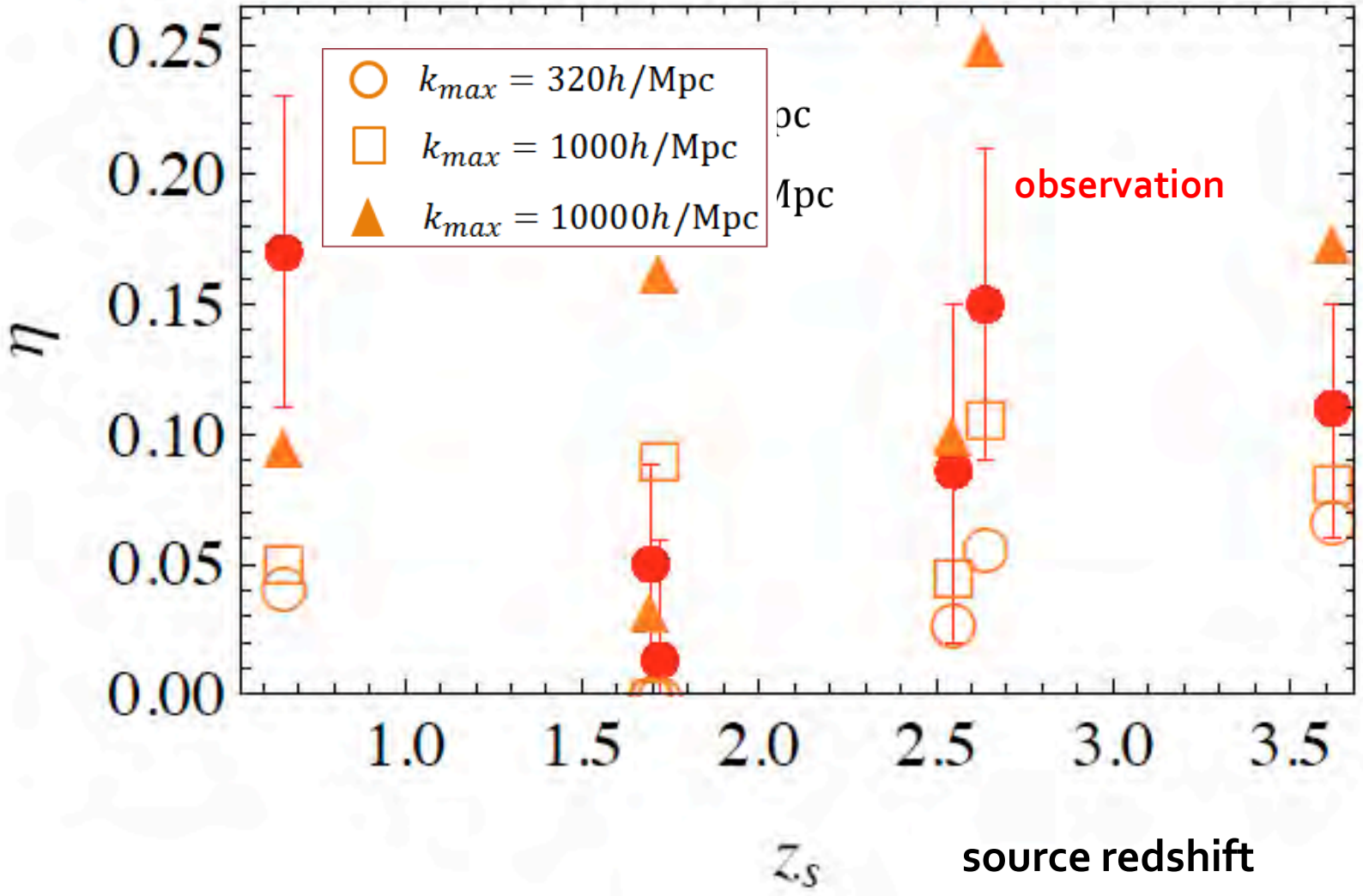
0.25
0.20
0.15
0.10
0.05
0.00
η
1.0
1.5
2.0
2.5
3.0
3.5
z_s
$k_{max} = 320h/\mathrm{Mpc}$
$k_{max} = 1000h/\mathrm{Mpc}$
$k_{max} = 10000h/\mathrm{Mpc}$
observation
source redshift

Summary

- Clustering line-of-sight halos with M=10^3-7 solar mass can explain the observed anomalous flux ratios without any substructures inside a lensing galaxy.

- The estimated amplitudes of convergence perturbation increase with the source redshift as predicted by theoretical models.

- Unique probe into mini-halos M<10^6 solar mass

Ray tracing simulation

L=10Mpc/h, Np=512^3, 1024^3 のシミュレーションボックスを並べる

下図の経路上で convergence & shear の摂動項 $\delta\kappa, \delta\gamma$ を計算（Born 近似）

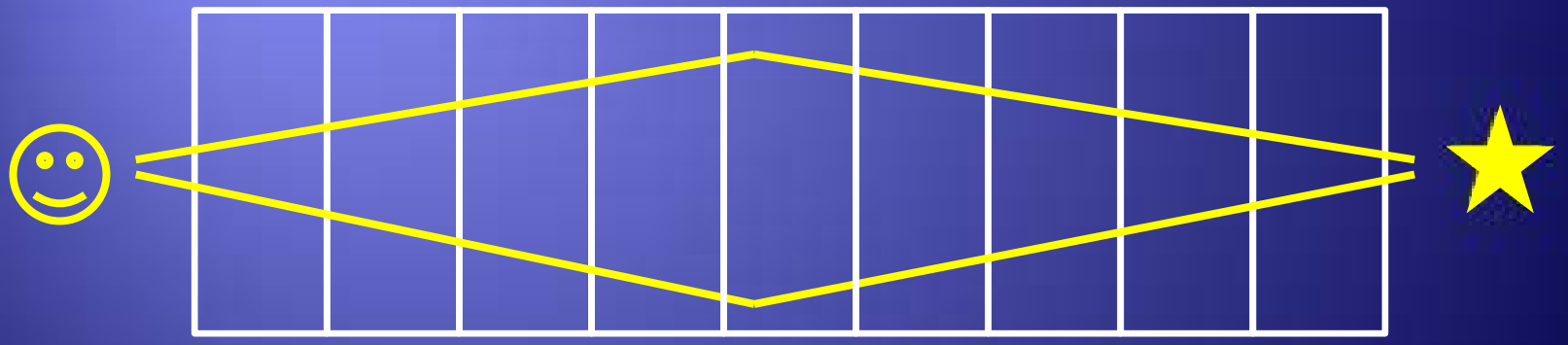

視野 4.8°×4.8°、 100 maps 用意

（浜名さん作成　Raytrix 使用）

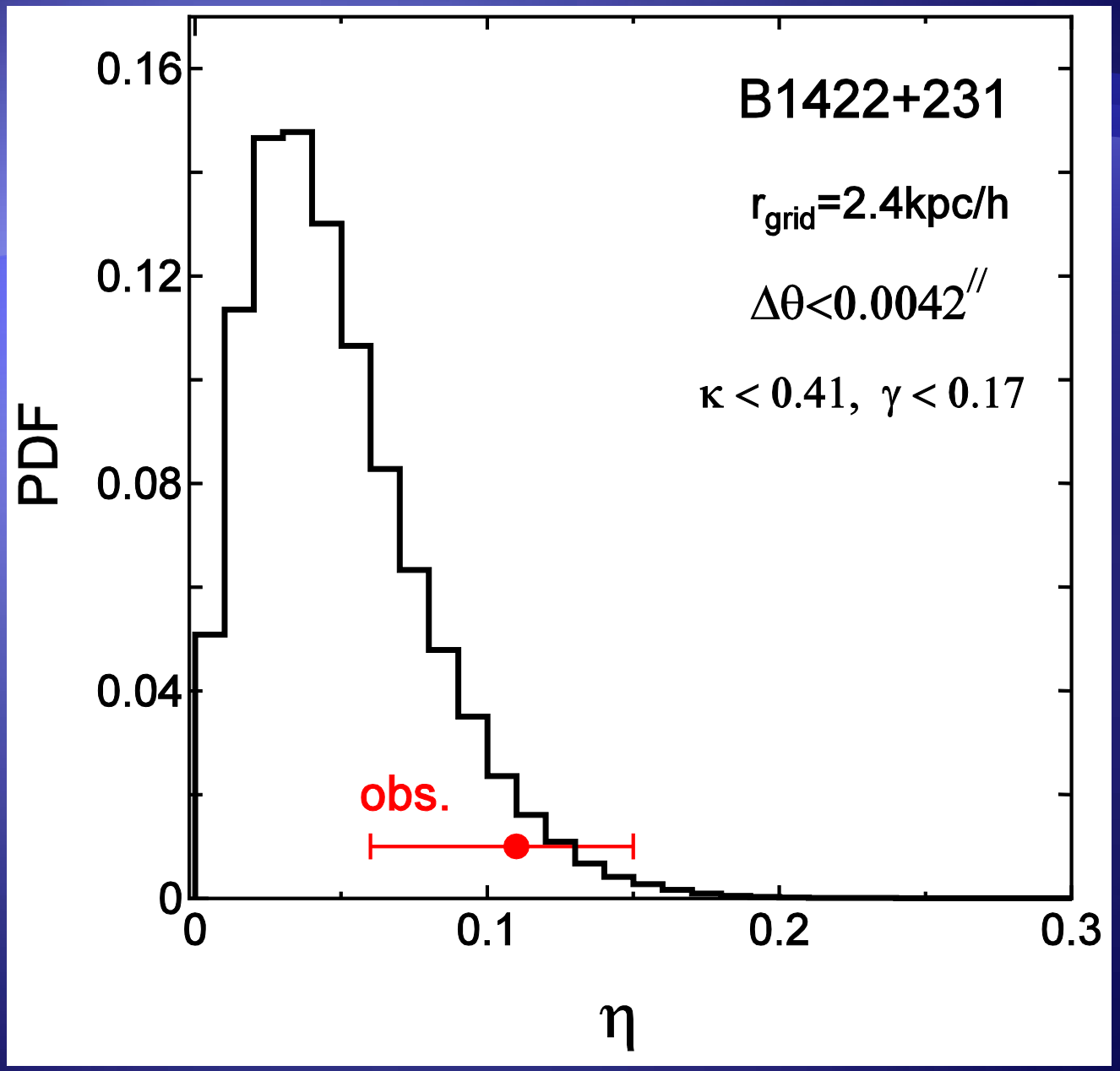
B1422+231
r_{grid}=2.4kpc/h
$\Delta\theta<0.0042''$
$\kappa < 0.41,\ \gamma < 0.17$
obs.
PDF
η
0.16
0.12
0.08
0.04
0
0
0.1
0.2
0.3

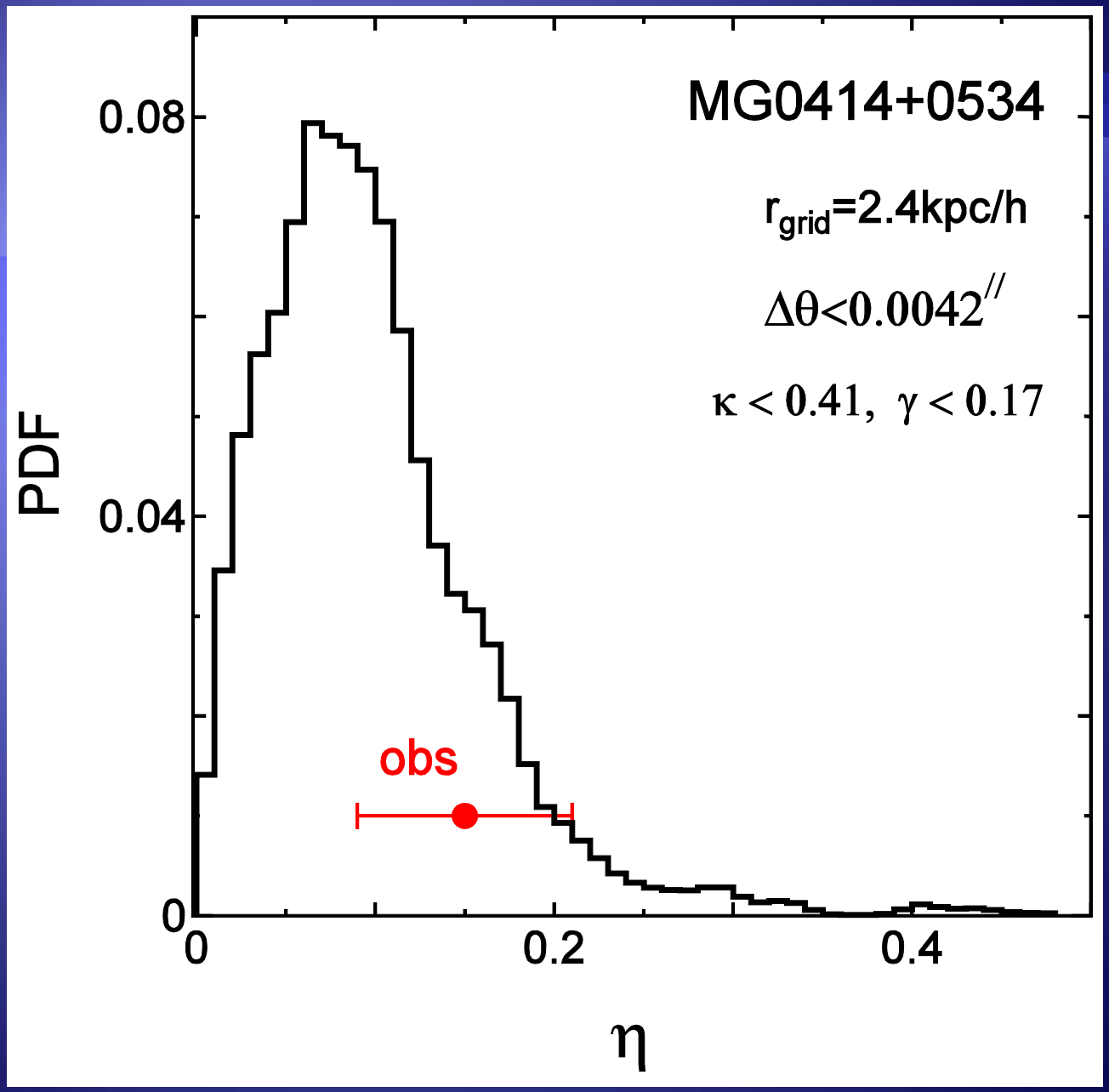
MG0414+0534
r_{grid}=2.4kpc/h
$\Delta\theta<0.0042''$
$\kappa < 0.41,\ \gamma < 0.17$
PDF
0.08
0.04
0
0
0.2
0.4
η
obs

Fitting function of non-linear matter power spectrum

Halo-fit model

～30% discrepancy

our model

<10% agreement

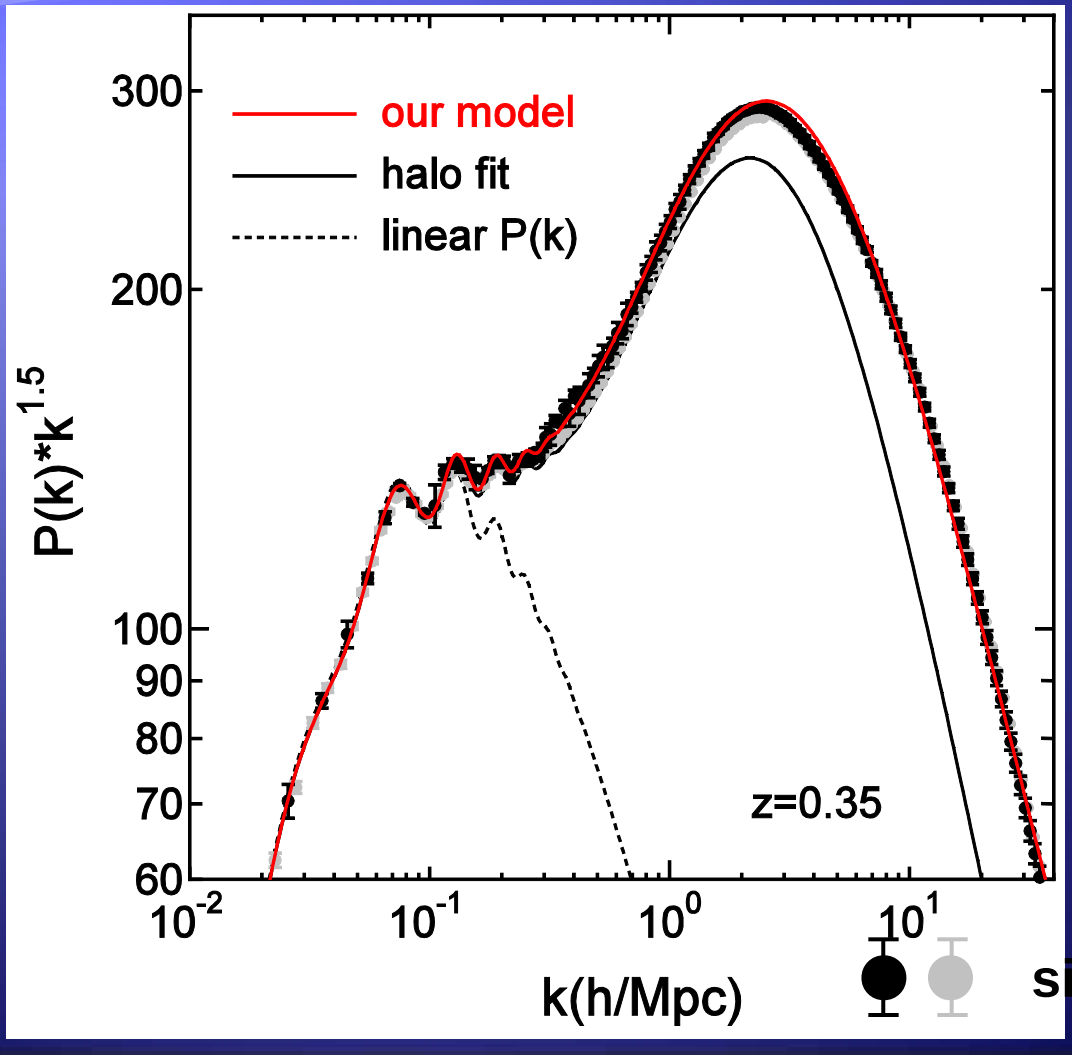

simulation results

Fitting function of non-linear matter power spectrum

Halo-fit model

～30% discrepancy

our model

<10% agreement

Cosmic shear, convergence power spectrum & correlation function

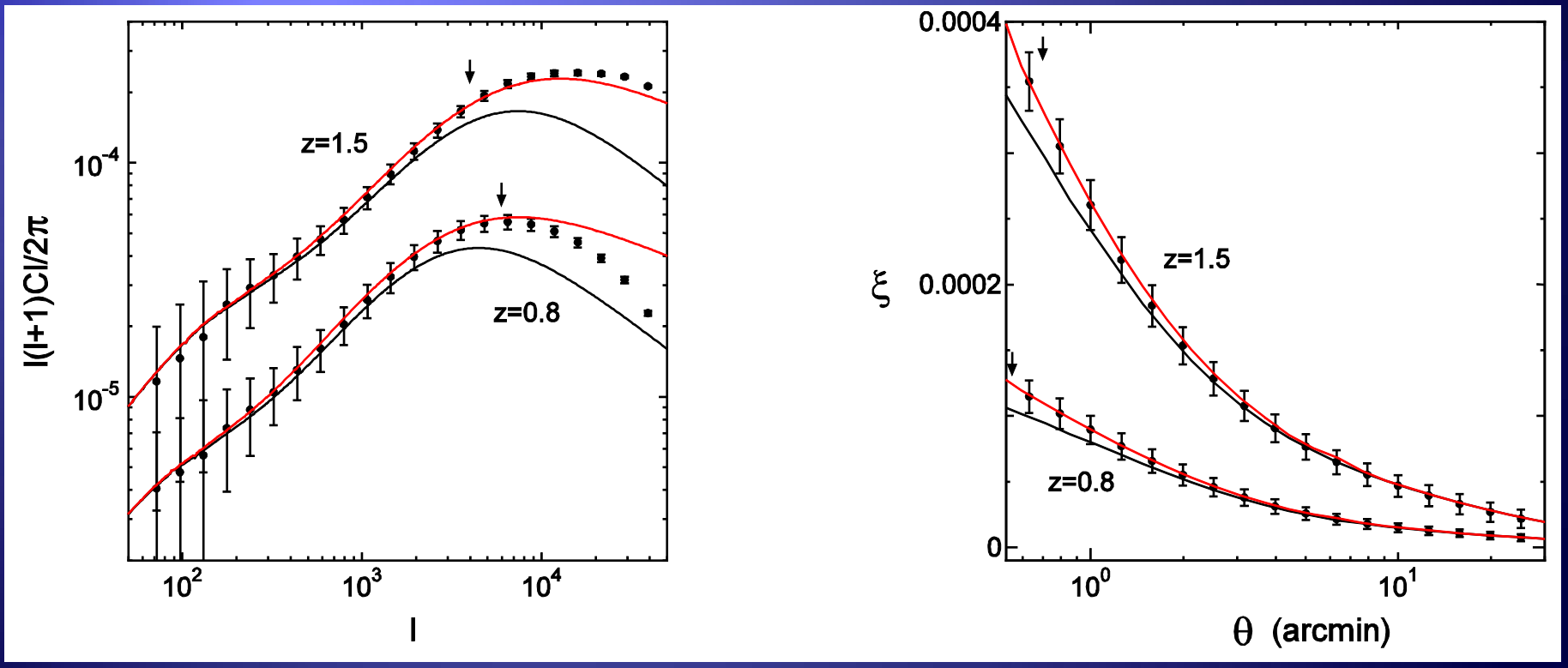

Fitting function of non-linear matter power spectrum

Halo-fit model

～30% discrepancy

our model

<10% agreement

Cosmic shear, convergence power spectrum & correlation function

RT, Sato, Nishimichi, Taruya, Oguri, 2012

arXiv:1208.2701

Non-linear P(k) の計算　変更した CAMB code 差し上げます

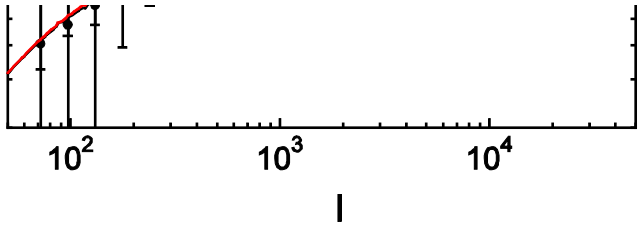

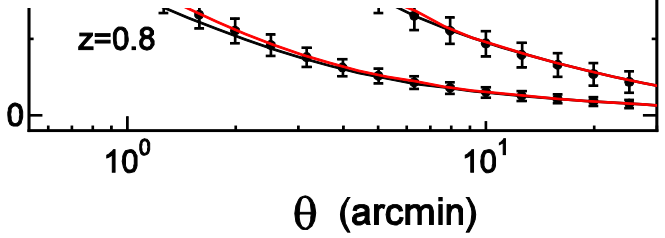

HSC用全天ray-tracing simulation　浜名さん、白埼君、吉田さん、、、

全天gravitational lensing ray-tracing開発

5) テスト結果 (nres=10, nside=1024, theta_res~3.4')

全天kappa map (zs=1)

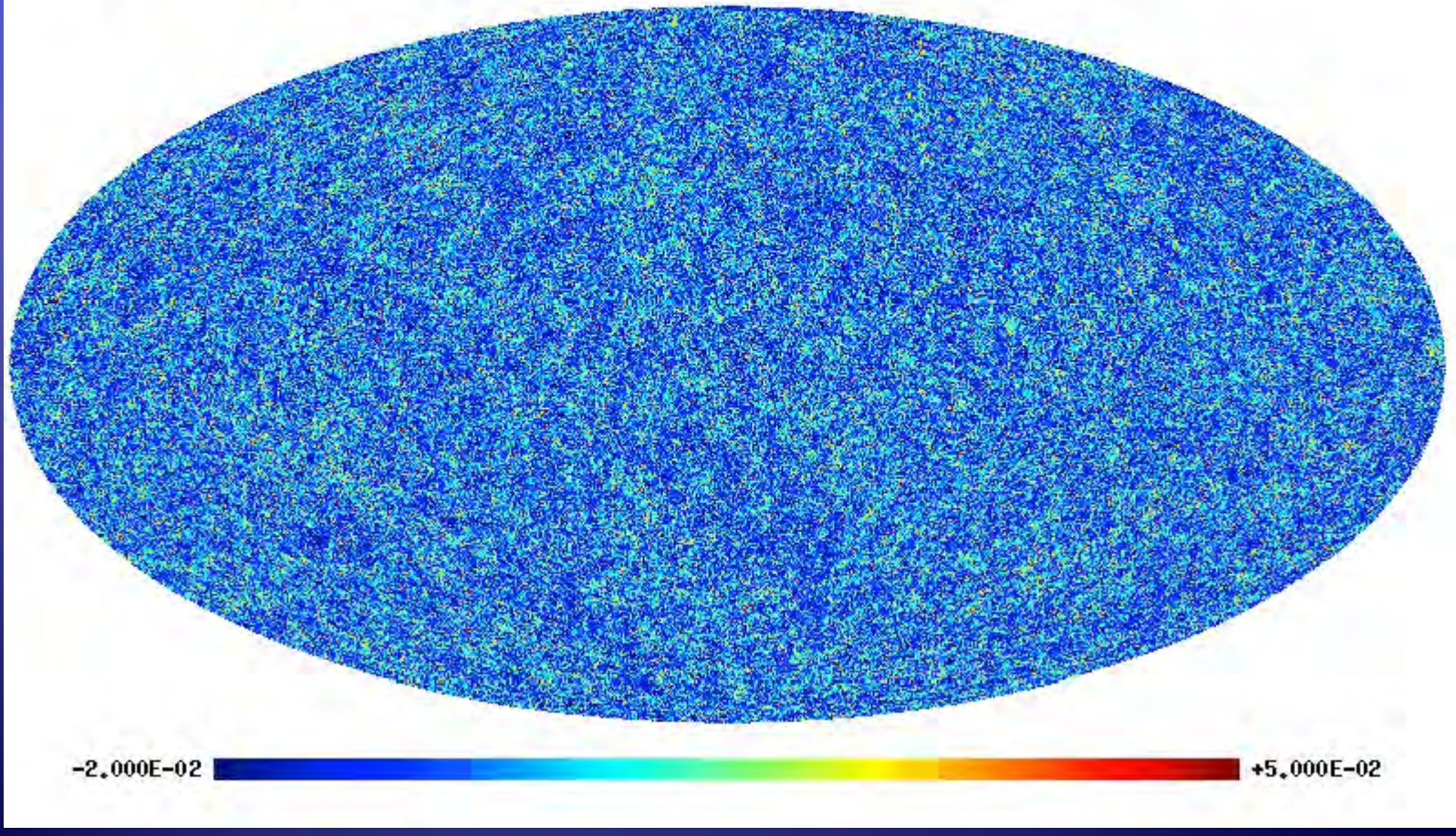

Future work

- Consistency check using light-ray tracing simulations (N(>2)-point correlation effects, etc.)
- Minimum change in astrometric shift for lensed image & lens.
- Check of SIE+ES, luminous group/satellite galaxies
- Extention to radio lenses incorporating finite source-size effects

Outline

- Introduction (flux ratio anomalies)
- Magnification perturbation
- Non-linear power spectrum
- Application to MIR lenses
- Summary
- Future work

Introduction

Suppression Mechanism

- Baryon physics (reionization, tidal disruption due to disk, SNe feedback)
- New physics (warm dark matter, self-interacting DMs, super WIMPs, non-trivial inflaton dynamics)
- Need to probe clustering property of halos with M<10^9 solar mass

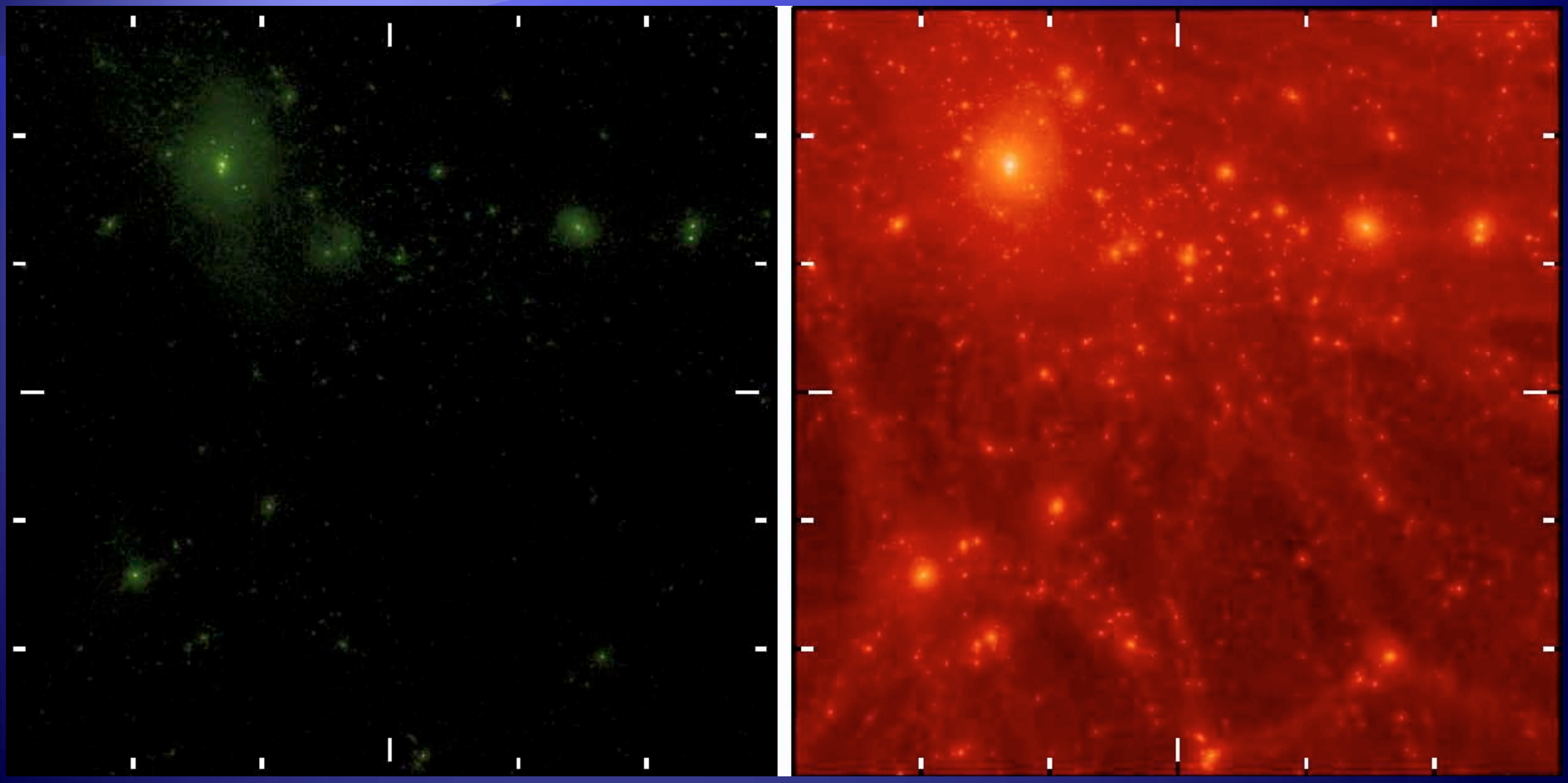

11.2 Mpc

Simulation by Sawara et al .2012

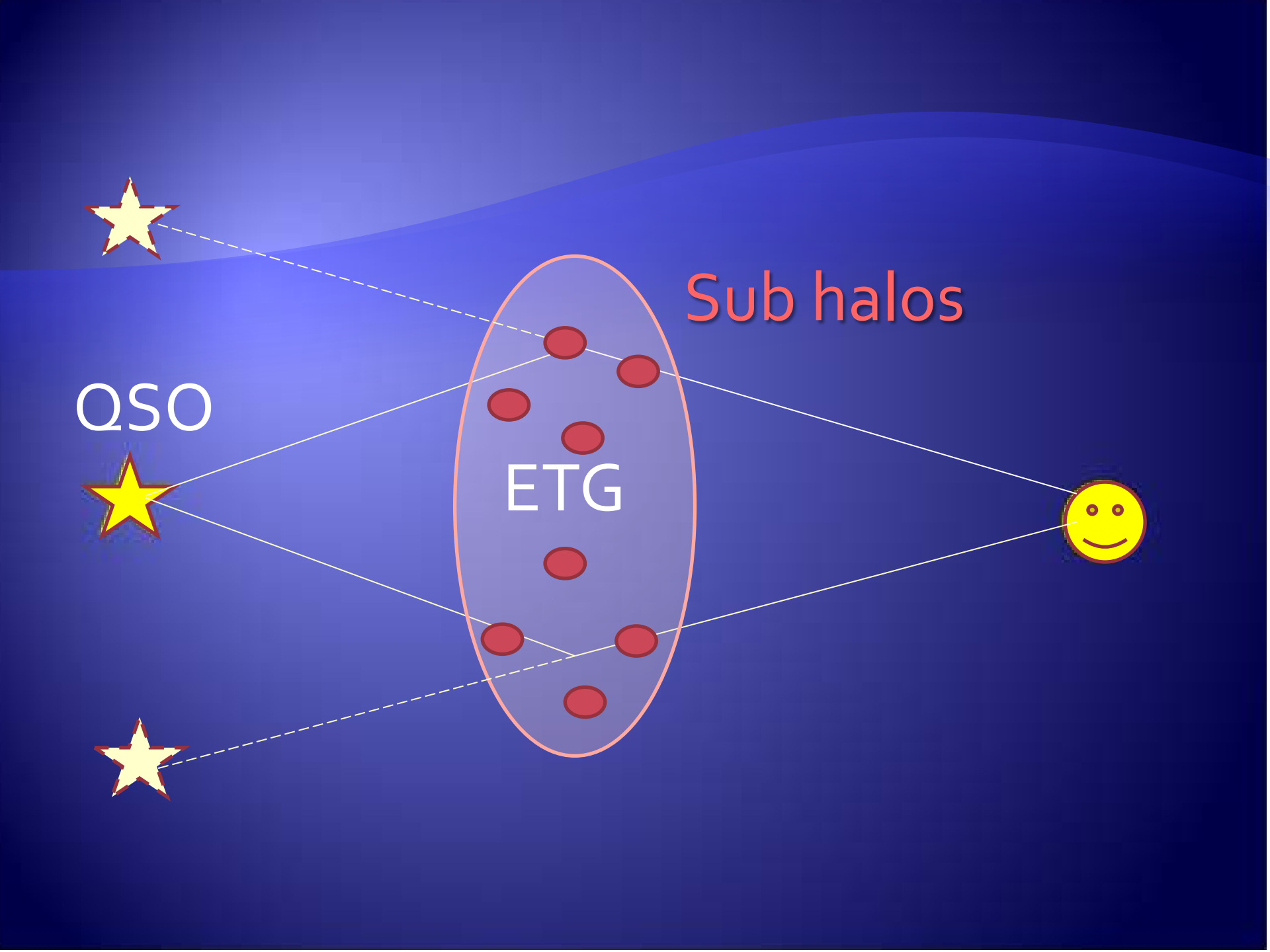
Sub halos
QSO
ETG

Missing Satellite Problem

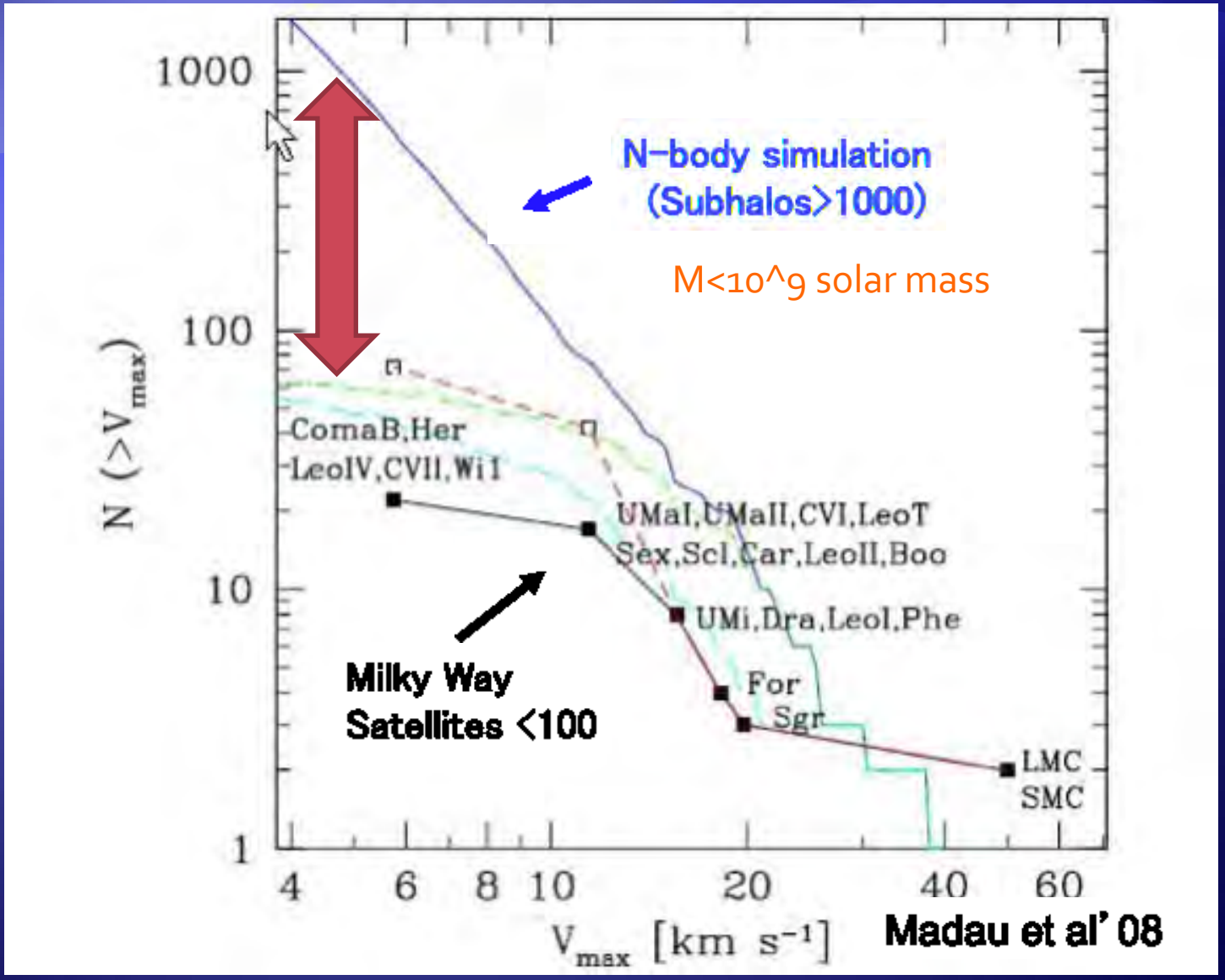

Parity of lensed images

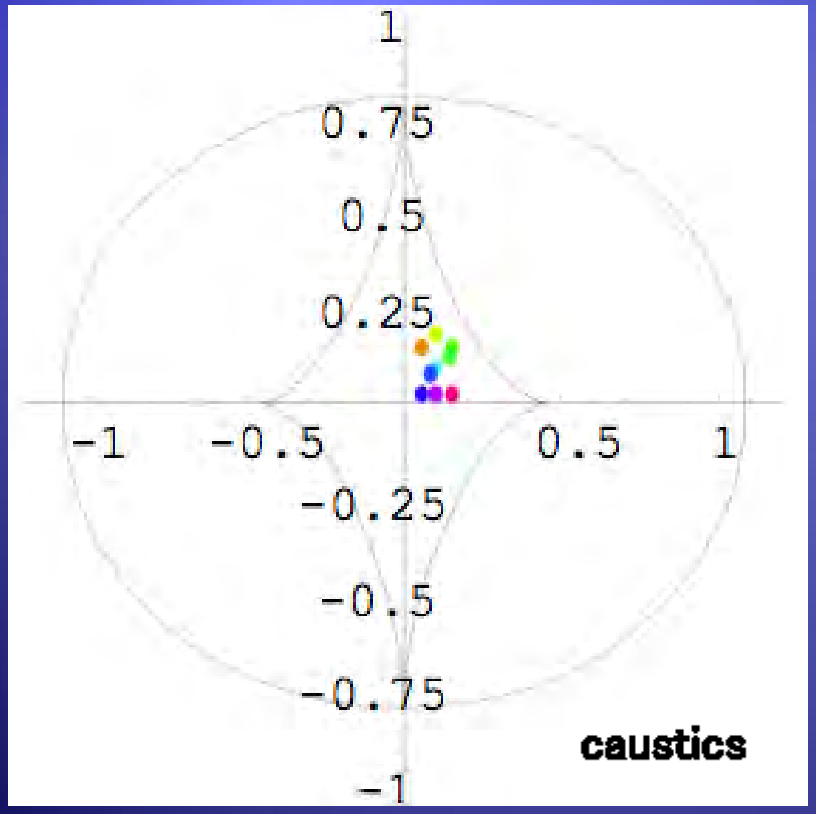

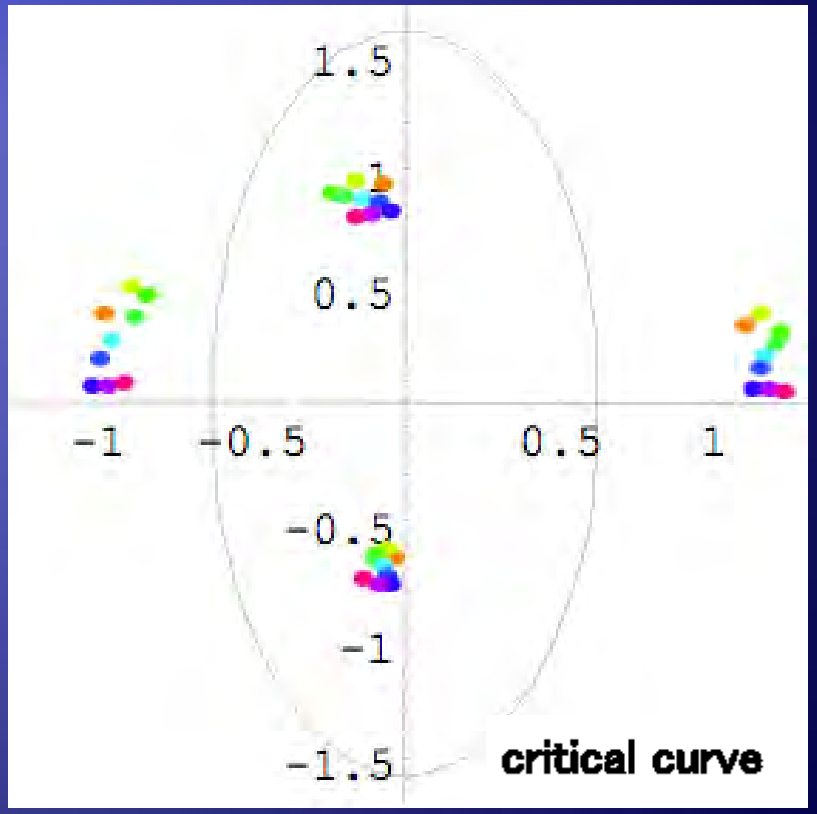

Systematic (de)magnification

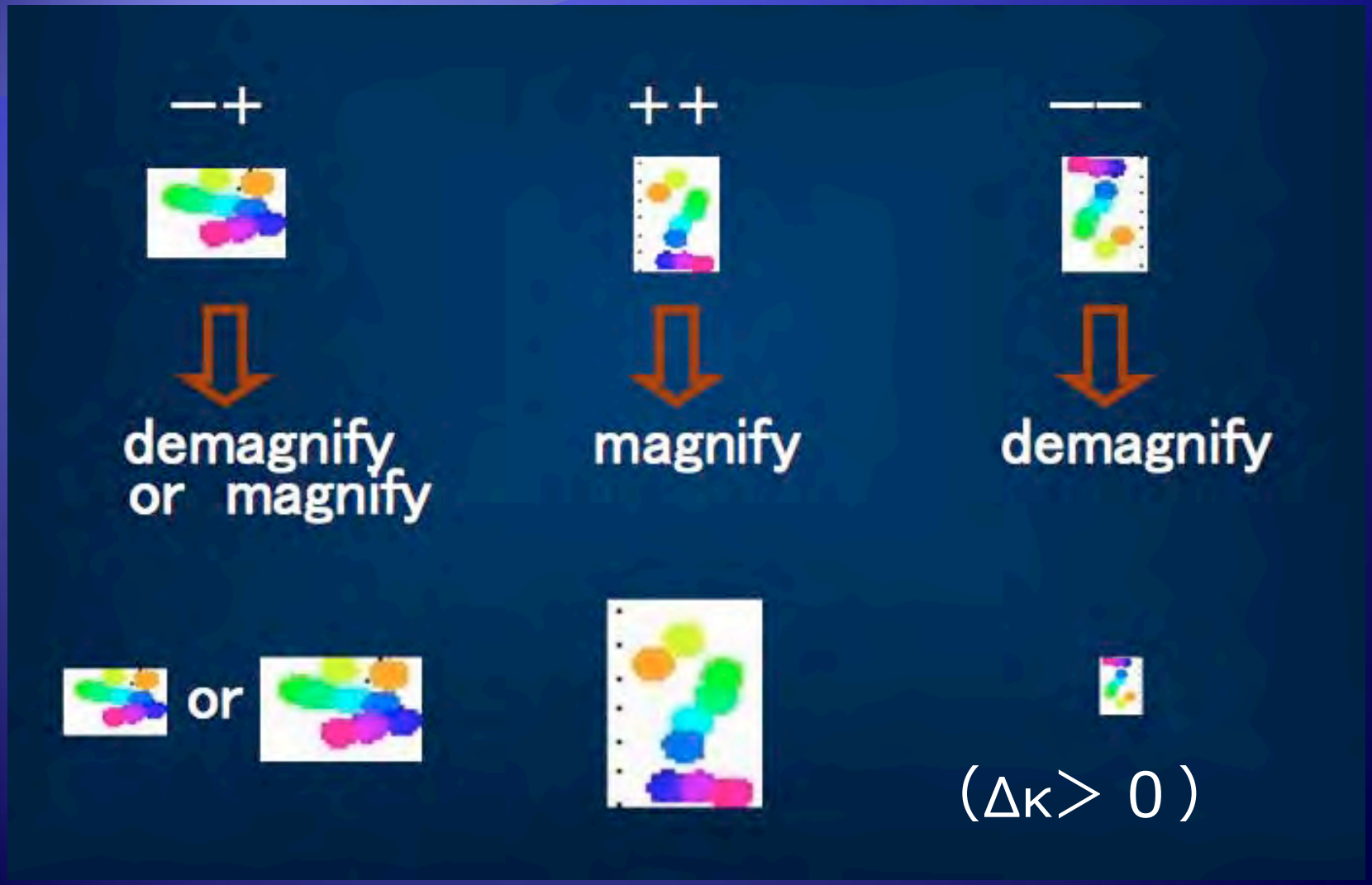

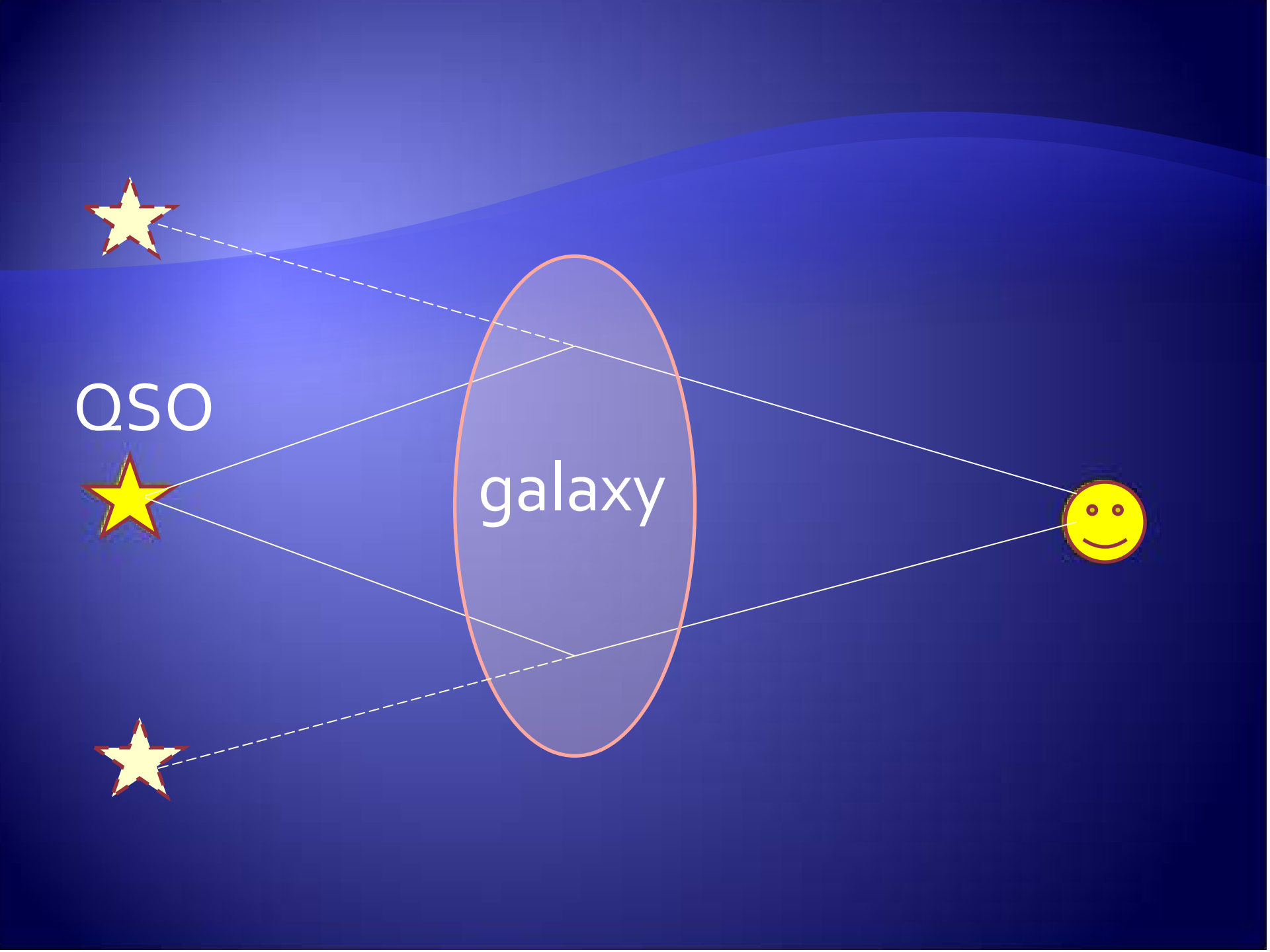
QSO
galaxy

MG0414+0534

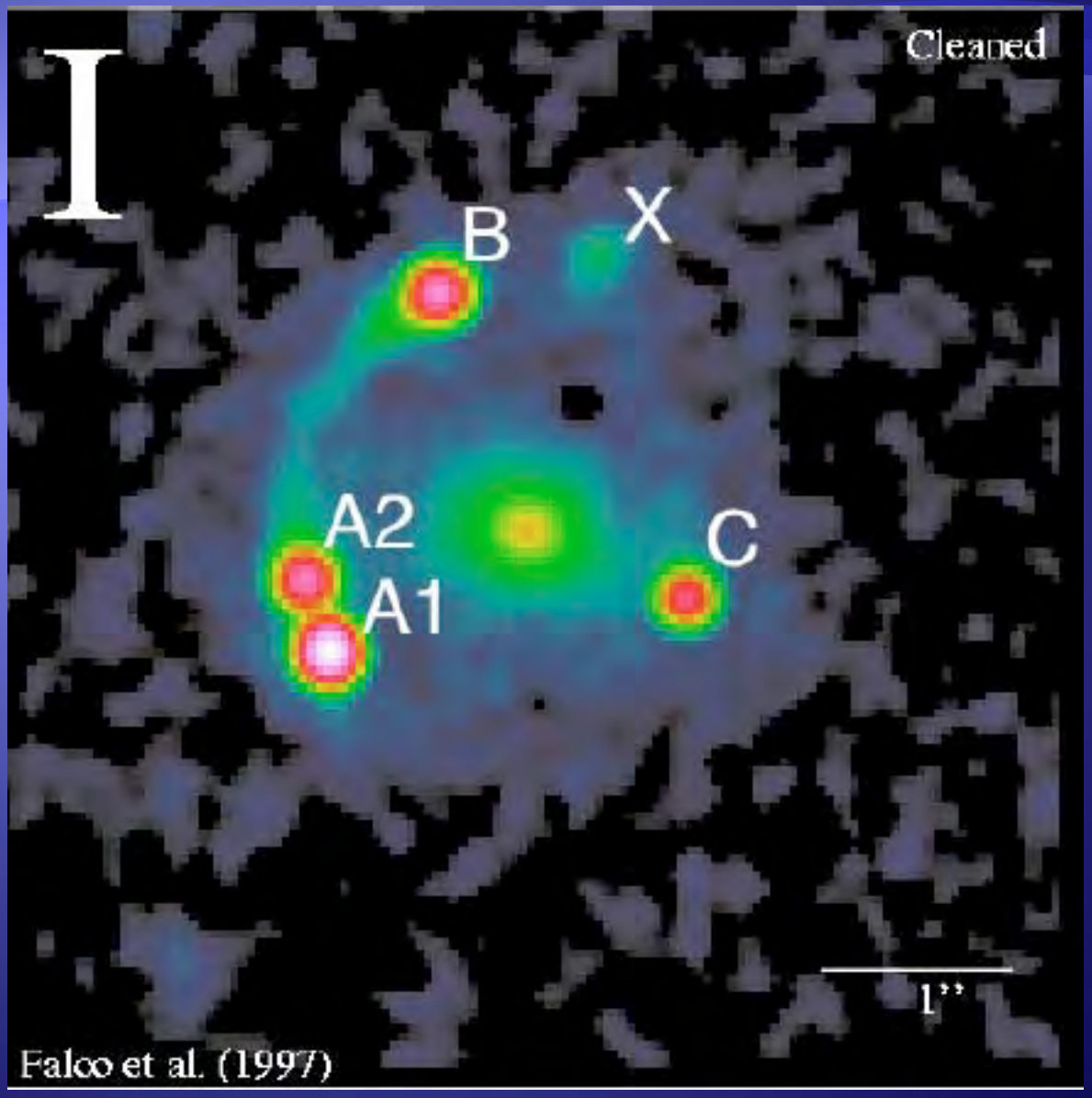

MG0414+0534

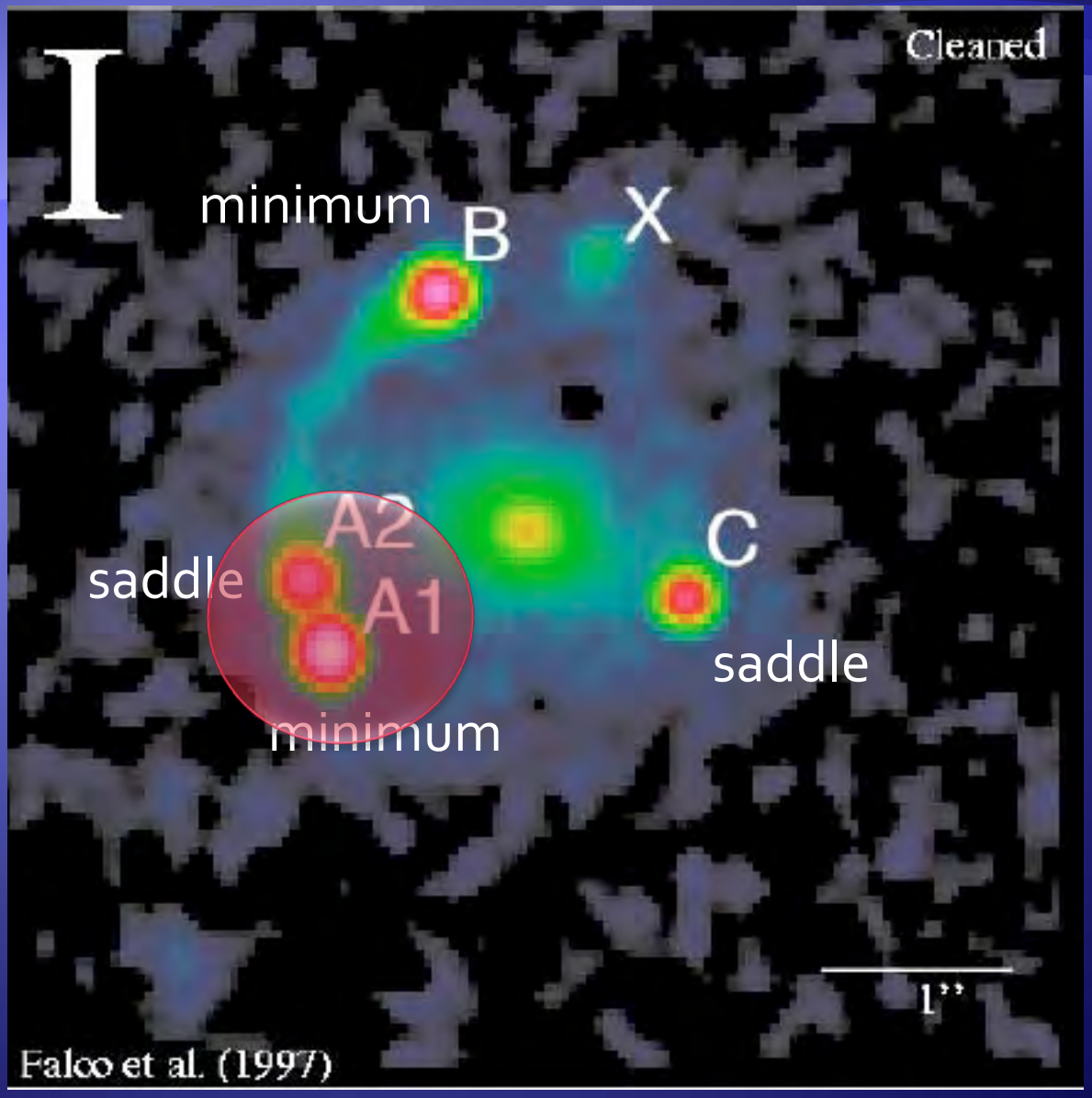
I
Cleaned
minimum
B
X
A2
saddle
A1
C
saddle
minimum
1''
Falco et al. (1997)

MG0414+0534

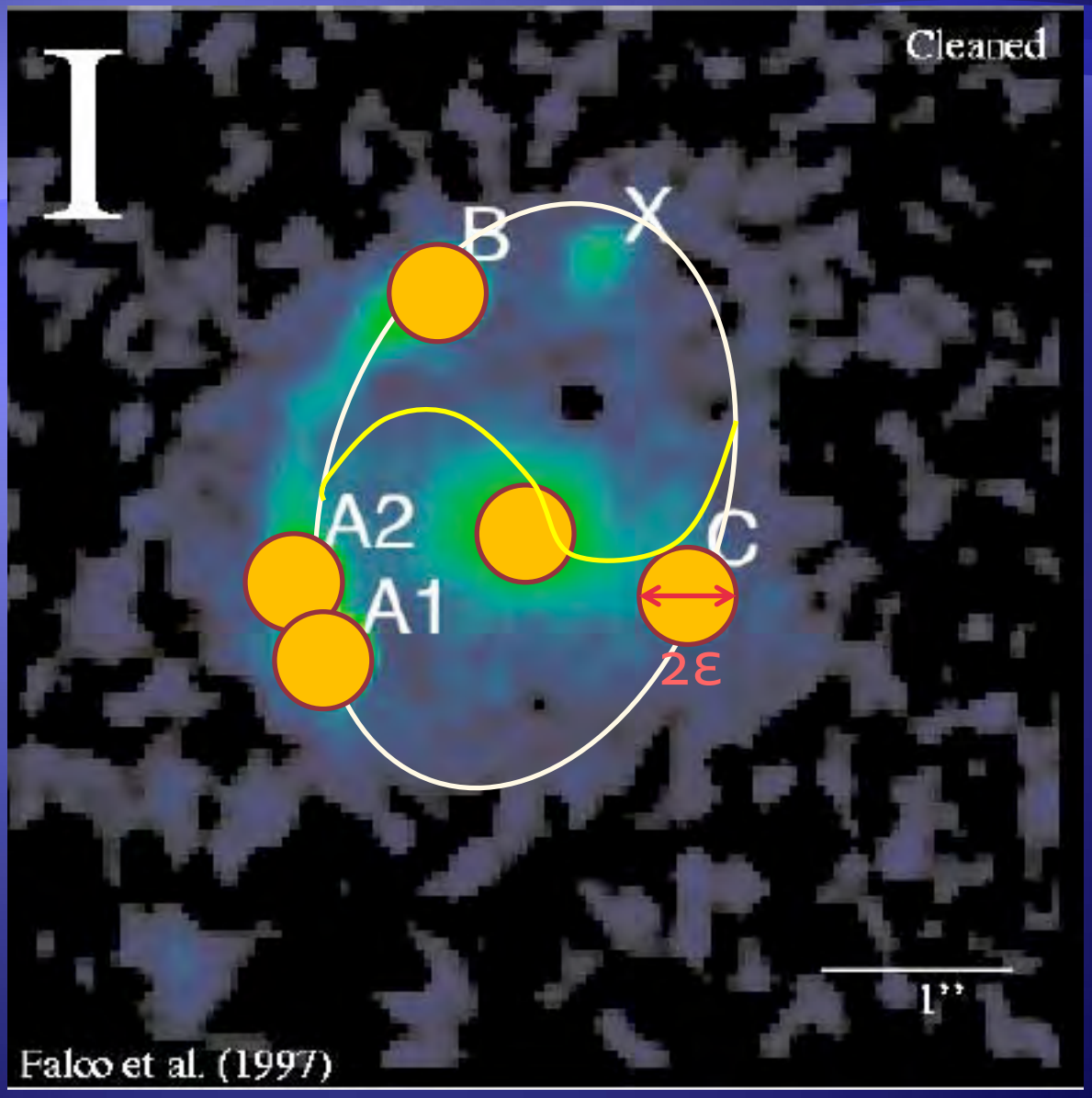

MG0414+0534

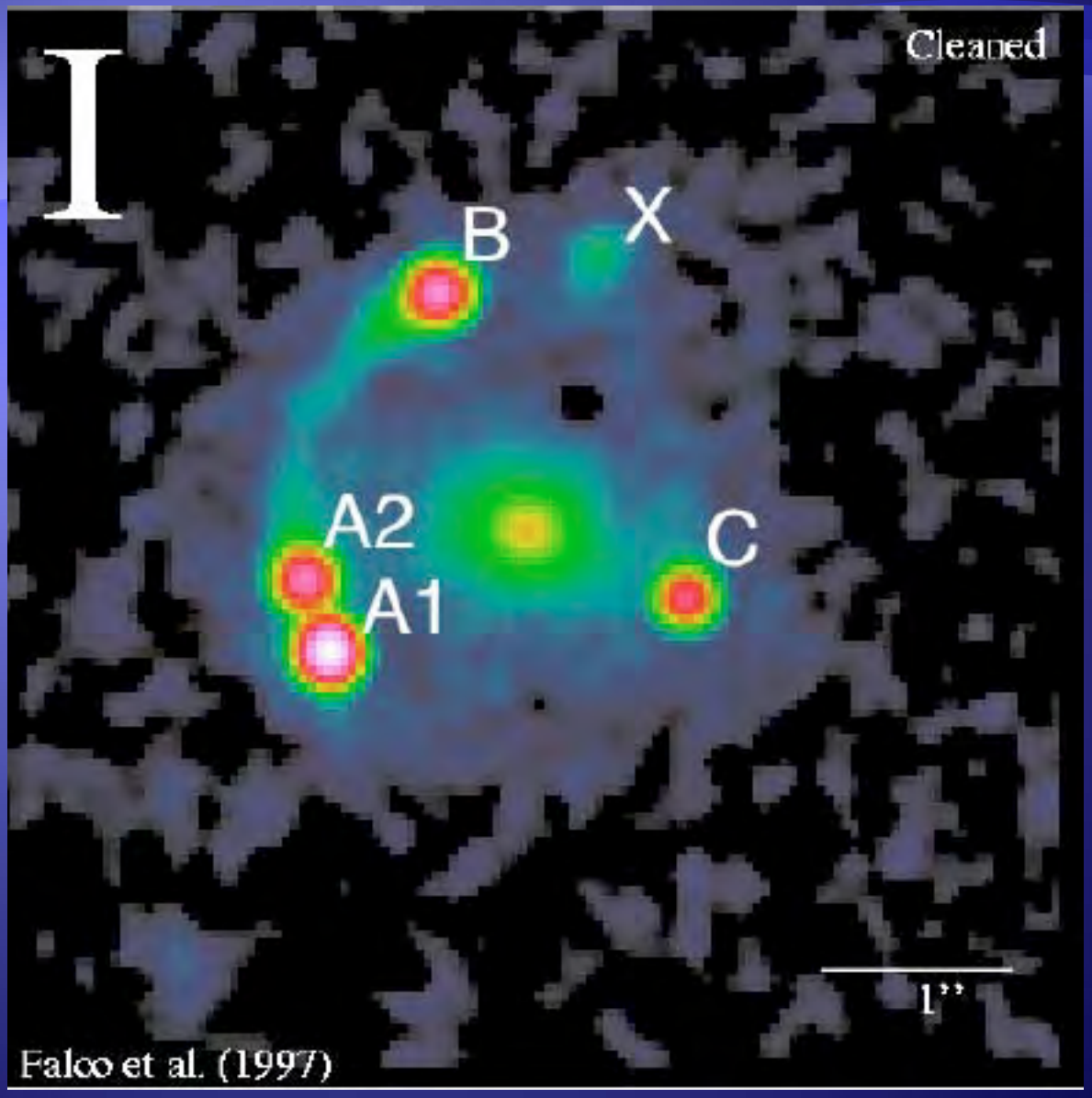

MIR quadruple lenses

Table 1. Observed MIR Flux Ratios

Lens	z_L	z_S	N	Flux Ratio			$\langle\epsilon\rangle$ ($''$)	$\langle\theta\rangle$ ($''$)	Reference
RXJ1131-1231($\star$)				A/B	C/B				
	0.295	0.658	3	$1.63^{+0.04}_{-0.02}$	$1.19^{+0.03}_{-0.12}$		0.017	1.9	1, 2
Q2237+0305				B/A	C/A	D/A			
	0.04	1.695	4	0.84 ± 0.05	0.46 ± 0.02	0.87 ± 0.05	0.0046	0.9	1, 3
PG1115+080				A2/A1					
	0.31	1.72	2	0.93 ± 0.06			0.020	1.2	1, 4
H1413+117				B/A	C/A	D/A			
	1.88($\star\star$)	2.55	4	0.84 ± 0.07	0.72 ± 0.07	0.40 ± 0.06	0.020	0.6	5
MG0414+0534				A2/A1	B/A1				
	0.96	2.639	3	0.90 ± 0.04	0.36 ± 0.02		0.0042	1.2	1, 3
B1422+231				A/B	C/B				
	0.34	3.62	3	0.94 ± 0.05	0.57 ± 0.06		0.0042	1.1	1, 4

References:1. CASTLES; 2. Sugai et al. 2007; 3. Minezaki et al. 2009; 4. Chiba et al. 2005; 5. MacLeod et al. 2009

Note: ($\star$): [OIII] line flux ratios. ($\star\star$): The lens redshift z_L is obtained from a best-fit model using the observed positions of the images and the primary lens, the flux ratios, and the time-delays between the images assuming $H_0 = 70\,\mathrm{km/s/Mpc}$.

Result II

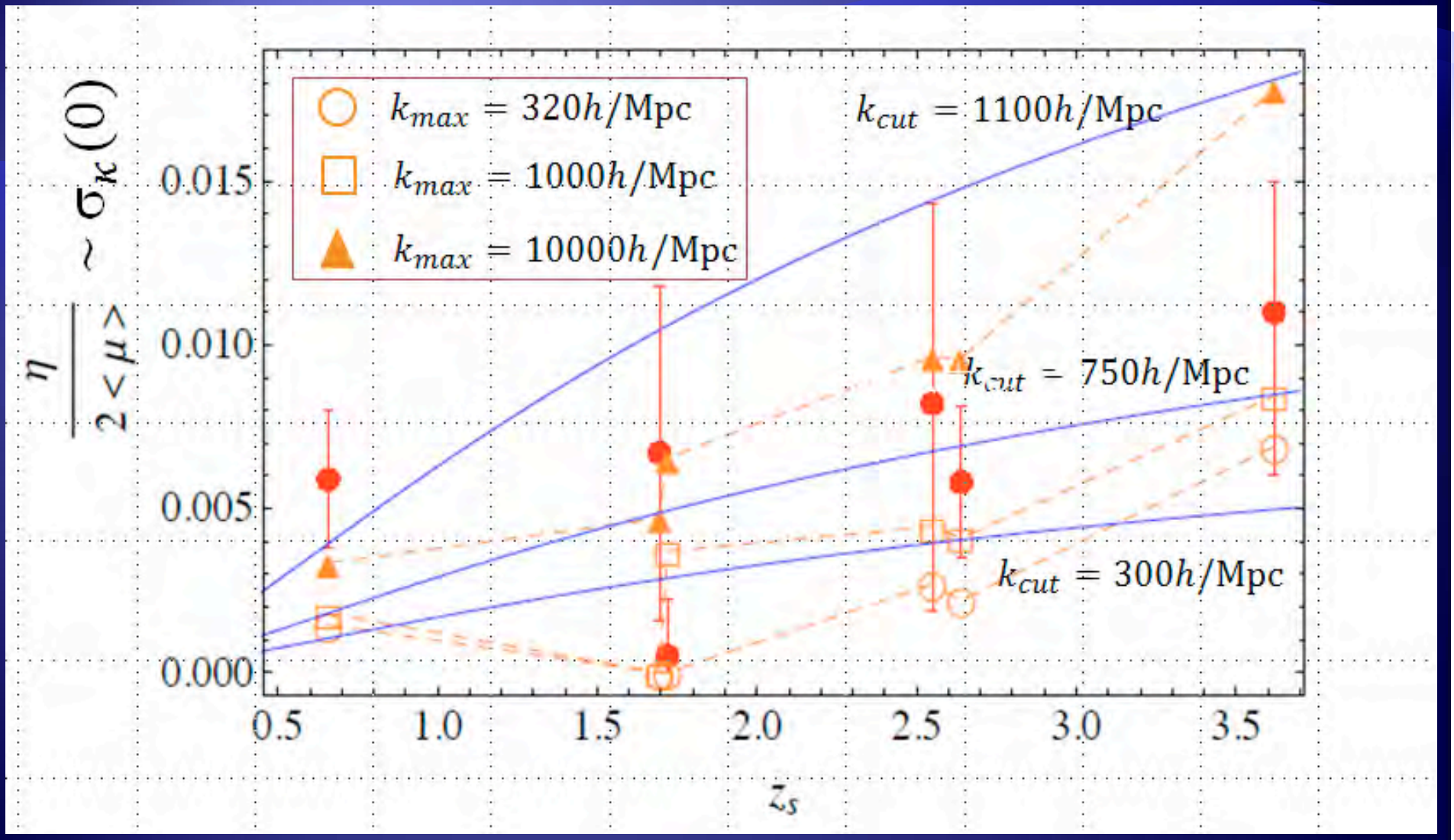
$\eta \left| \frac{\sim \sigma_\kappa(0)}{2 < \mu >} \right.$
$k_{max} = 320h/\mathrm{Mpc}$
$k_{max} = 1000h/\mathrm{Mpc}$
$k_{max} = 10000h/\mathrm{Mpc}$
$k_{cut} = 1100h/\mathrm{Mpc}$
$k_{cut} = 750h/\mathrm{Mpc}$
$k_{cut} = 300h/\mathrm{Mpc}$
0.015
0.010
0.005
0.000
0.5
1.0
1.5
2.0
2.5
3.0
3.5
z_s

MG0414+0534

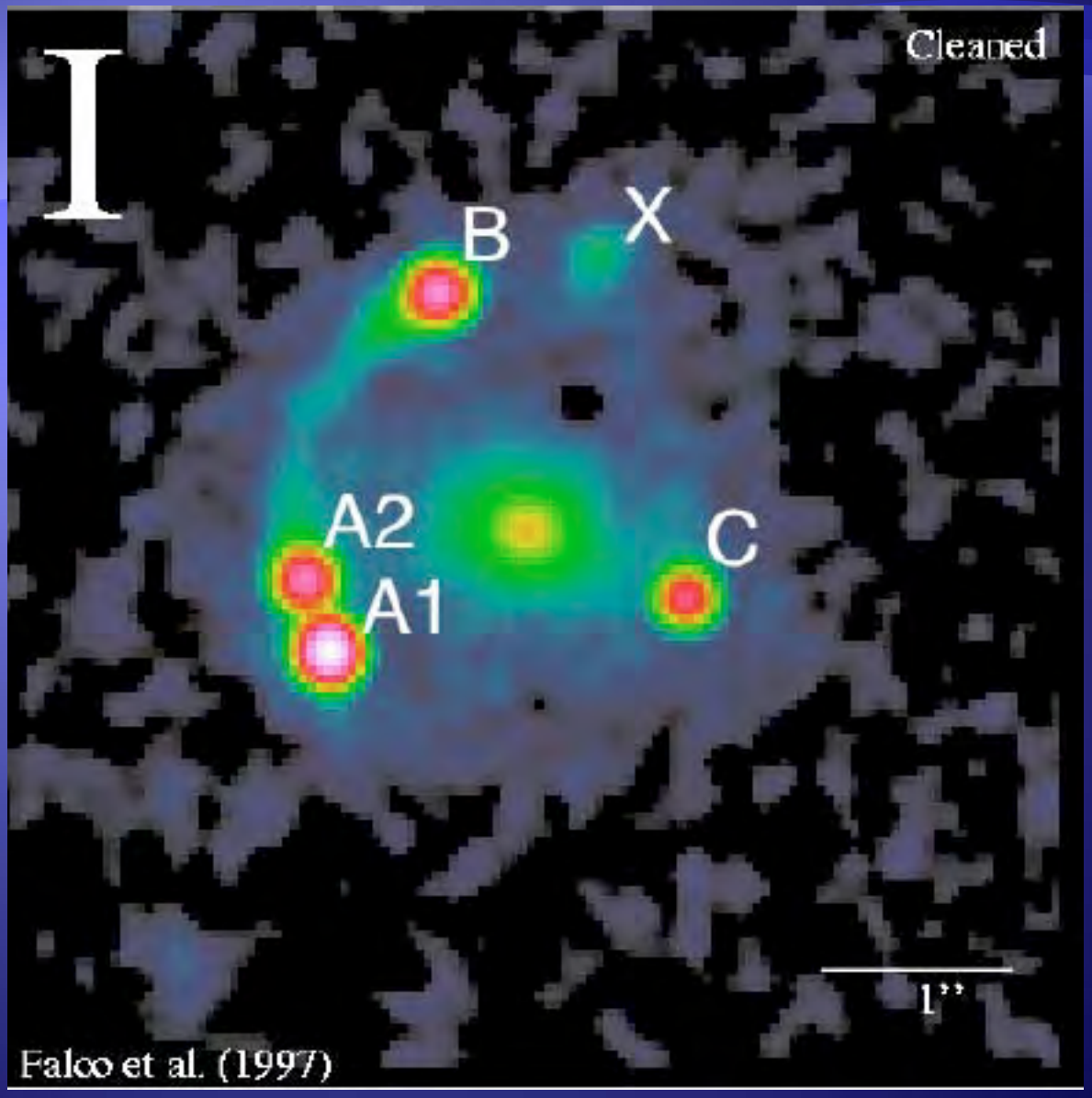

MG0414+0534

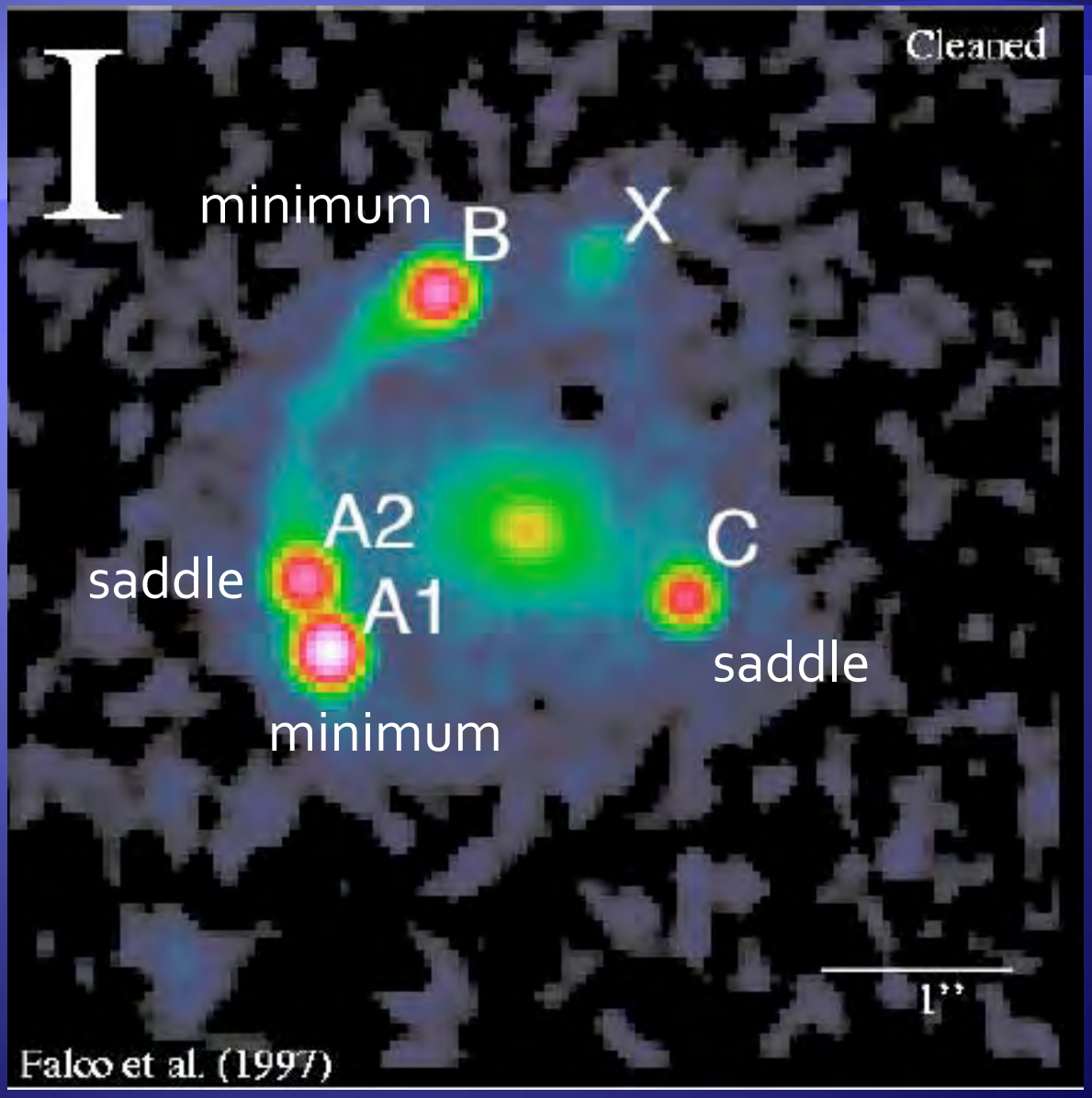
I
Cleaned
minimum
B
X
A2
saddle
A1
C
saddle
minimum
1''
Falco et al. (1997)

Astrometric shifts

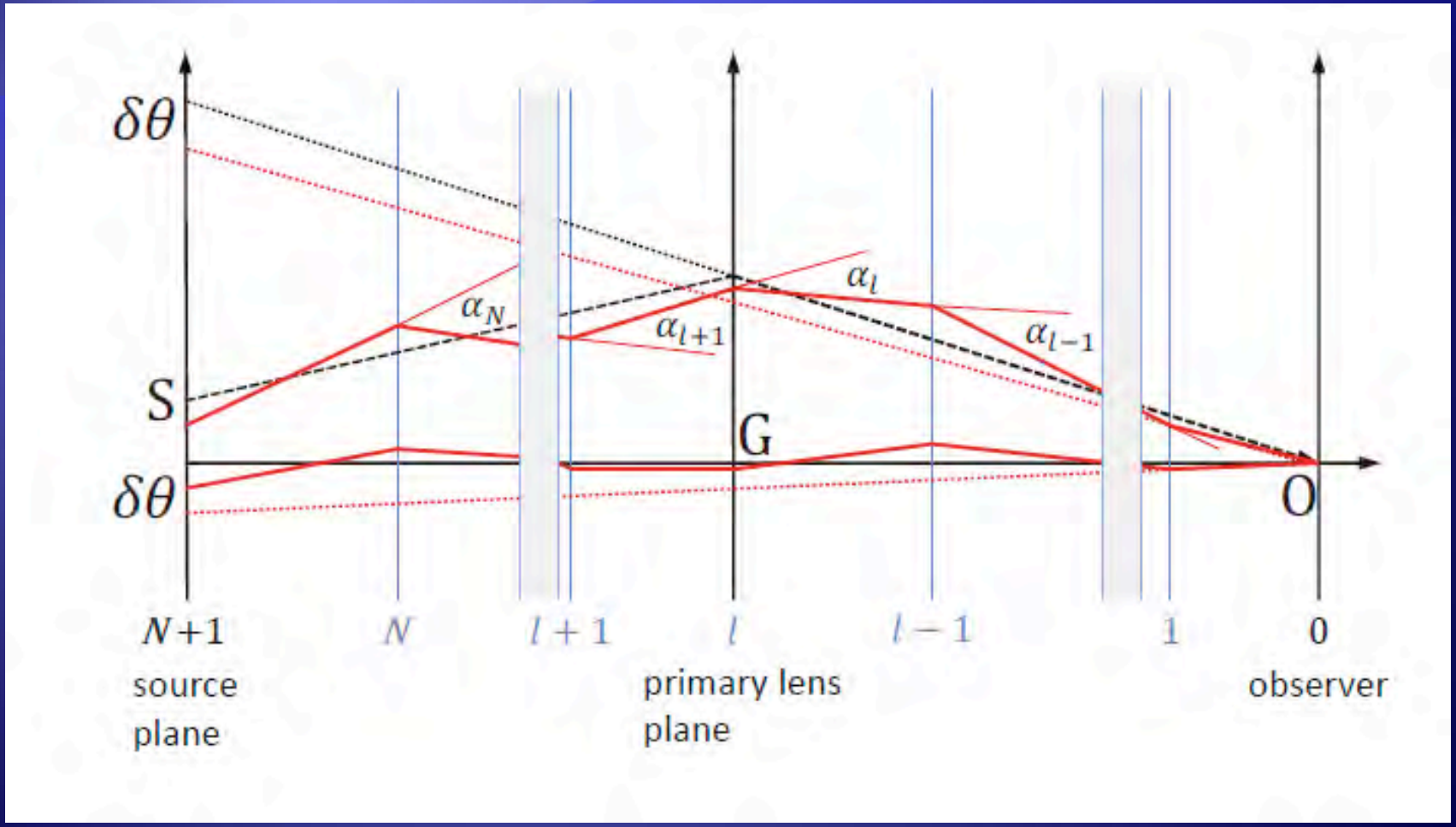

Astrometric shifts

2-point correlation in shift of image separated by θ

$$\xi_{\delta\theta}(\theta) \equiv \langle \delta\theta(0)\delta\theta(\theta) \rangle$$

Given by power spectrum P(k)

Astrometric shifts

$$k_{lens} \equiv 2\pi / L_{lens} \text{ where } L_{lens} \sim 4r(z_L)\theta_E$$

Minimum wavenumber given by the size of Einstein radius

$$k_{lens} = O[100 - 1000h / \mathrm{Mpc}]$$

Astrometric shifts

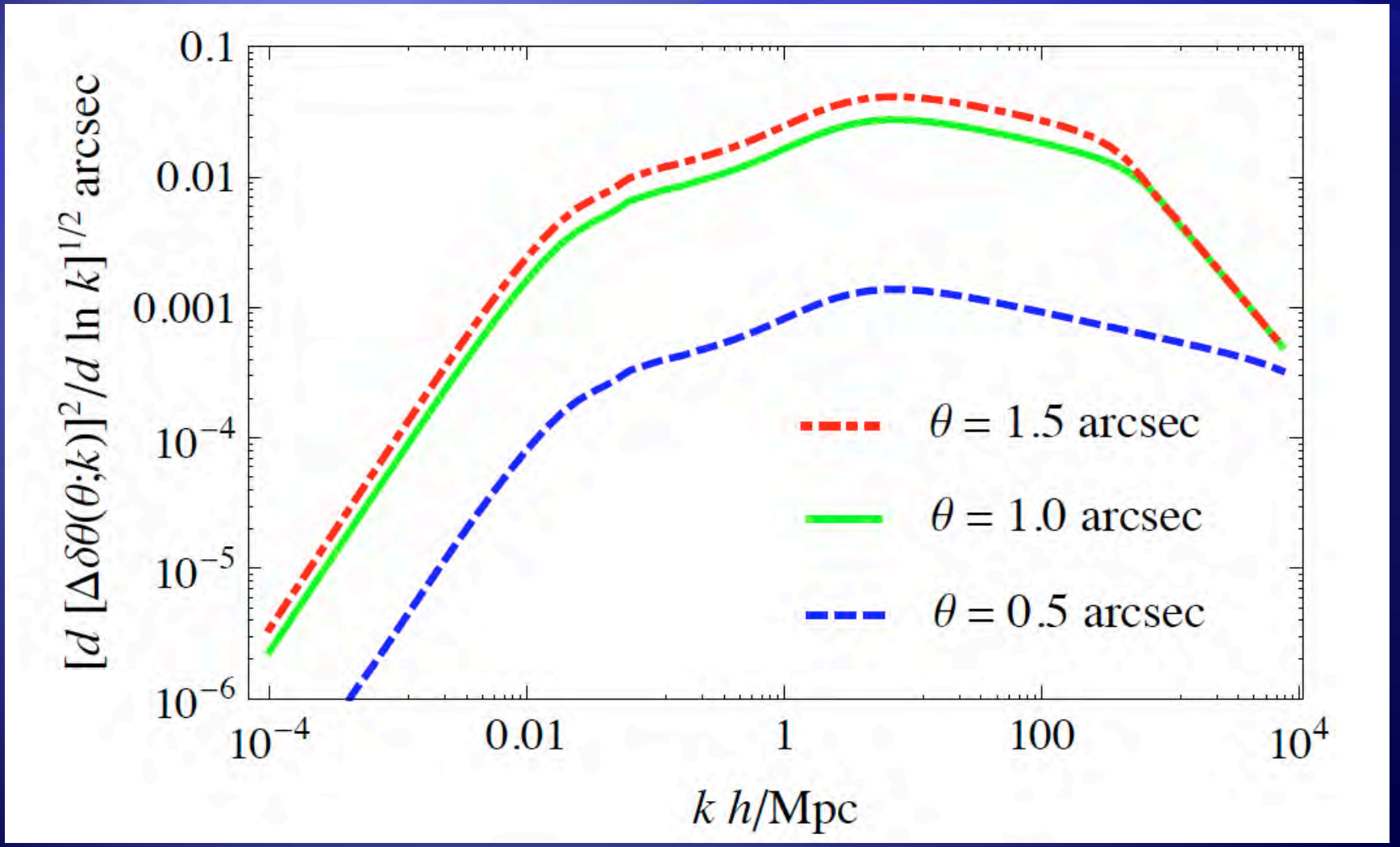

Astrometric shifts

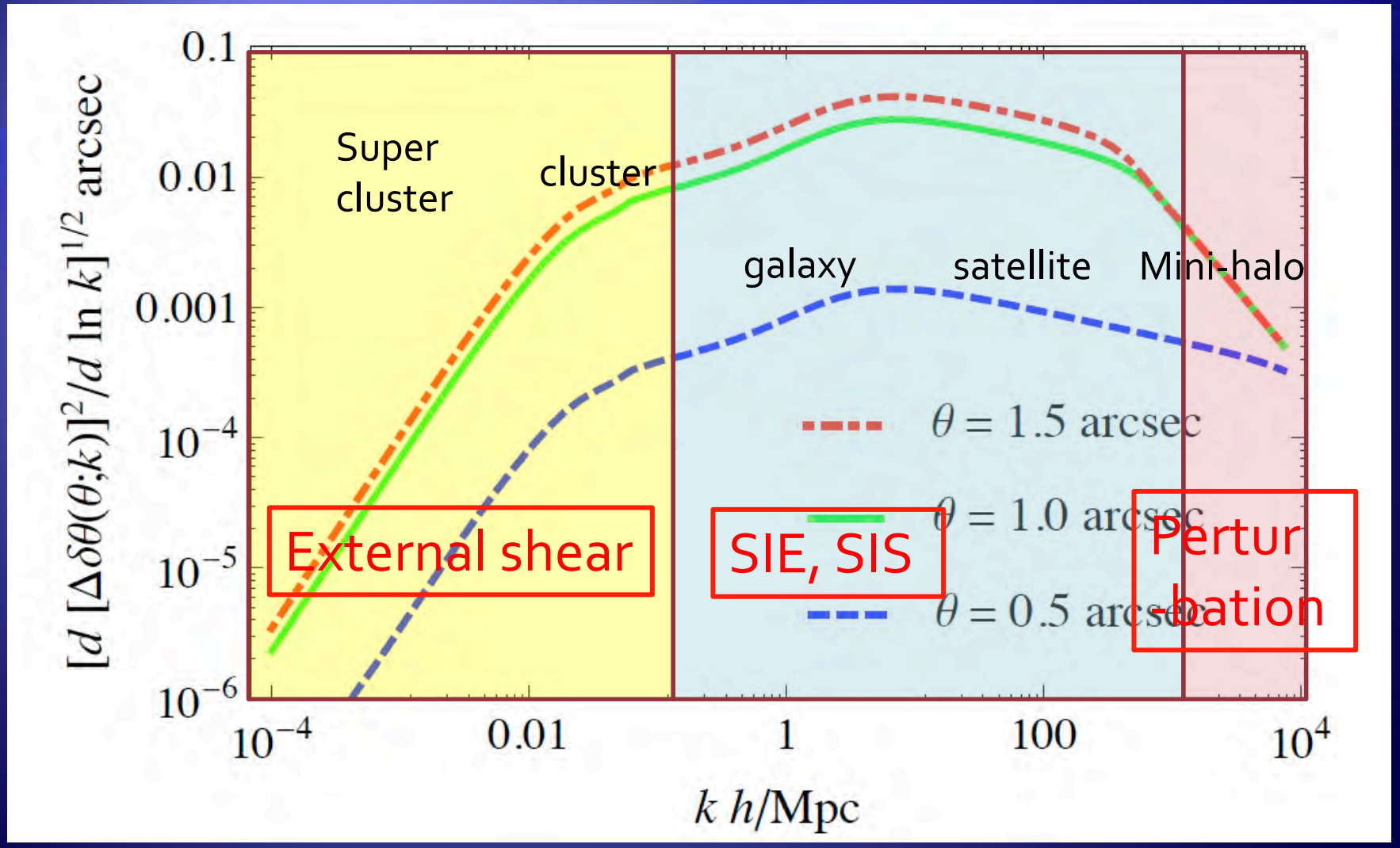

Constrained convergence power

- Accuracy in position of lensed images & lens k_ε
- Size of Einstein ring k_{lens}

$$k_{\min} = \mathrm{Min}[k_\varepsilon, k_{lens}]$$

Constrained r.m.s. convergence

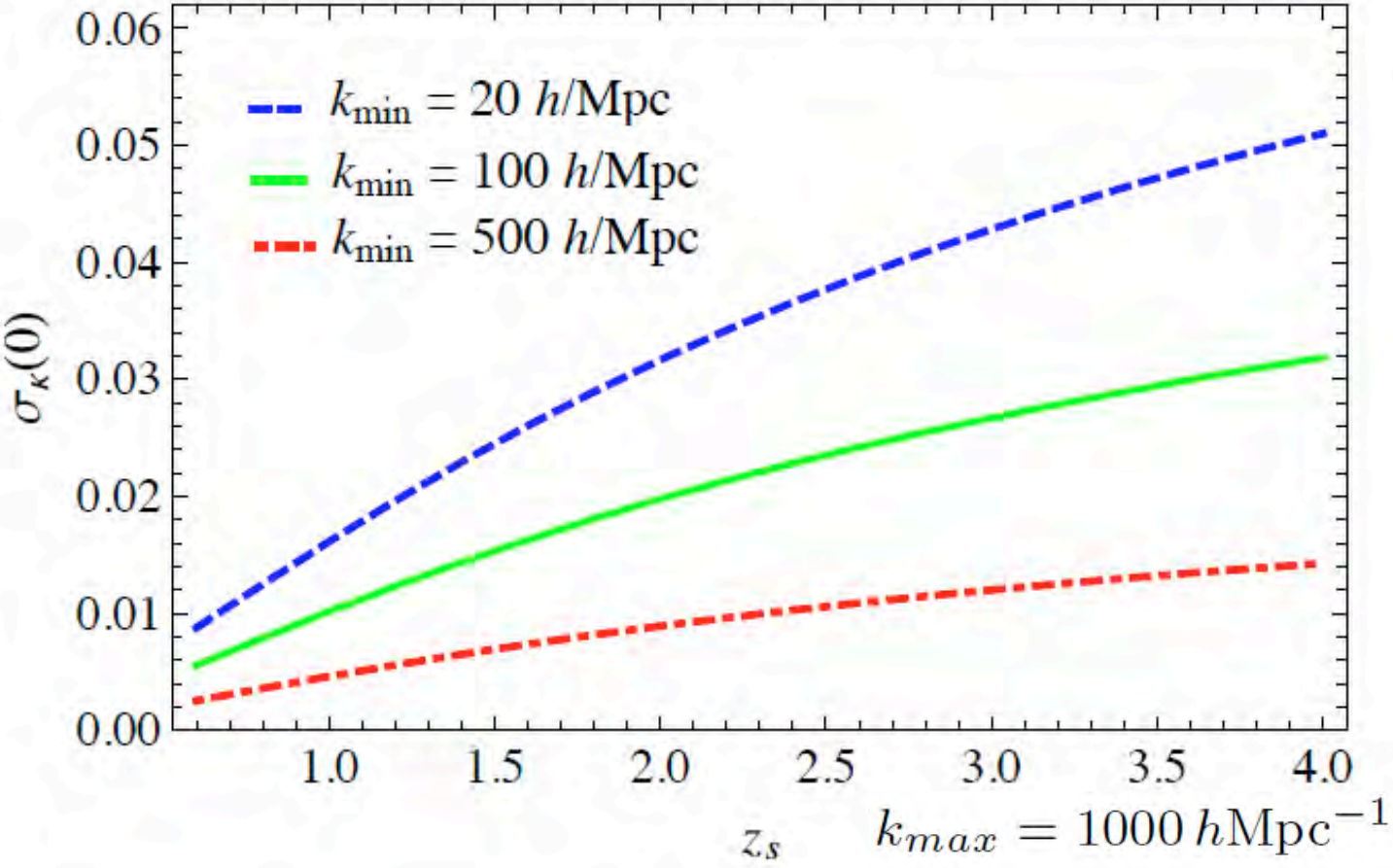

MIR quadruple lenses

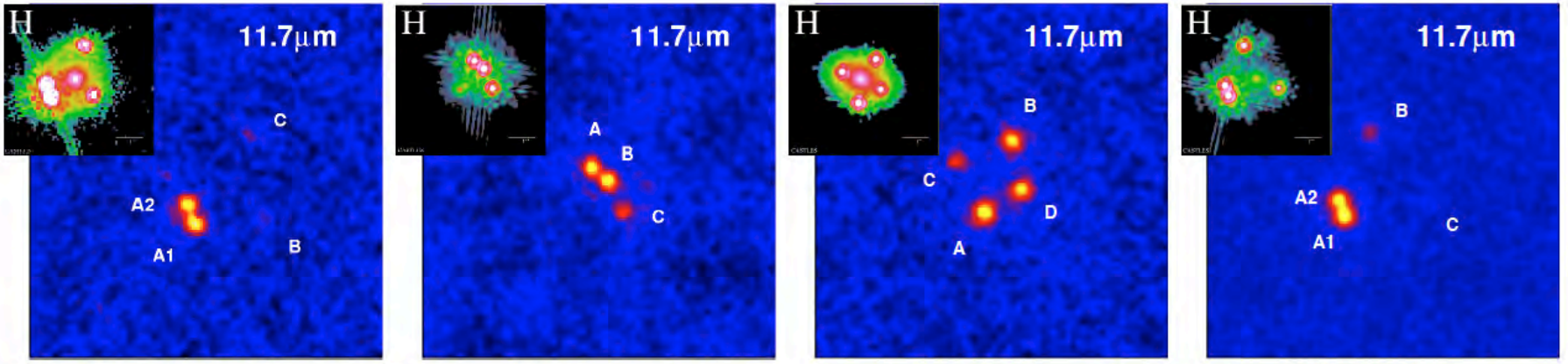

Figure 2: The mid-infrared images of quadruply lensed QSOs obtained by COMICS attached on Subaru telescope. From left to right, PG1115+080, B1422+231, Q2237+030, and MG0414+0534. The insets are their HST images for comparison (taken from CASTLES, http://cfa-www.harvard.edu/glensdata/).

- Source size estimated from dust reverberation method ~ 1~3pc >>Einstein radius of stars

(by Chiba et al 2005 & Minezaki et al. 2009)